

An Assessment of Visual Testing

Pacific Northwest National Laboratory

**U.S. Nuclear Regulatory Commission
Office of Nuclear Regulatory Research
Washington, DC 20555-0001**



An Assessment of Visual Testing

Manuscript Completed: November 2004
Date Published: November 2004

Prepared by
S.E. Cumblidge, M.T. Anderson, S.R. Doctor

Pacific Northwest National Laboratory
902 Battelle Blvd.
Richland, WA 99352

D.A. Jackson and W.E. Norris, NRC Project Managers

Prepared for
Division of Engineering Technology
Office of Nuclear Regulatory Research
U.S. Nuclear Regulatory Commission
Washington, DC 20555-0001
NRC Job Code Y6604



Abstract

In response to increasing interest from nuclear utilities in replacing some volumetric examinations of nuclear reactor components with remote visual testing, the Pacific Northwest National Laboratory has examined the capabilities of remote visual testing for the Nuclear Regulatory Commission. This report describes visual testing and explores the visual acuities of the camera systems used to examine nuclear reactor components. The types and sizes of cracks typically found in nuclear reactor components are reviewed. The current standards in visual testing are examined critically, and several suggestions for improving these standards are proposed. Also proposed for future work is a round robin test to determine the effectiveness of visual tests and experimental studies to determine the values for magnification and resolution needed to reliably image very tight cracks.

Contents

Abstract.....	iii
Executive Summary.....	ix
Foreword.....	xi
Acknowledgments.....	xii
Abbreviations.....	xiii
1 Introduction.....	1.1
2 The Visual Testing Technique.....	2.1
3 Service-Related Cracking in Nuclear Reactor Components.....	3.1
3.1 Surface Appearance of Common Cracks in Reactor Components.....	3.1
3.2 Factors Influencing a Crack Opening Dimension.....	3.4
3.3 Compiled Crack Opening Dimensions for Cracks in Austenitic Stainless Steel	3.5
4 Remote Visual Testing in the Nuclear Industry.....	4.1
4.1 Overview.....	4.1
4.2 Examples of Remote Visual Tests.....	4.2
4.3 Probability of Crack Detection vs. Crack Opening Dimension.....	4.7
5 Discussion.....	5.1
5.1 Crack Opening Dimensions.....	5.1
5.2 Resolution and Acuity Standards for Visual Testing Equipment	5.1
5.3 Resolution Testing and the Modulation Transfer Function.....	5.6
5.4 Scanning Technique.....	5.7
5.5 A Comparison of Visual and Ultrasonic Testing.....	5.8
6 Conclusions.....	6.1
7 Recommendations.....	7.1
8 References.....	8.1
Appendix A- Supplemental Photographs of Samples.....	A.1
Appendix B- Specifications for DIAKONT and EVEREST VIT Visual Testing Systems .	B.1

Figures

Figure 2.1	Pixelation of line (a) into lower-contrast image (b).....	2.3
Figure 3.1	25- μm (0.001-in.) COD Mechanical Fatigue Crack in Stainless Steel.....	3.2
Figure 3.2	Two 15- μm (0.0005-in.) COD Thermal Fatigue Cracks on Machined..... Stainless Steel Surface .	3.3
Figure 3.3	Two Views of 125- μm (0.005-in.) COD Stress Corrosion Crack..... along Weld in Stainless Steel.	3.4
Figure 3.4	Two Stress Corrosion Cracks in Locking Bolt (100X magnification)..... (Morrin et al. 1978)	3.5
Figure 3.5	Crack Opening Dimension Distribution for Fatigue Cracks (Ekström..... and Wåle 1995)	3.6
Figure 3.6	Crack Opening Dimension Distribution for Stress Corrosion Cracks.....	3.7
Figure 3.7	Crack Opening Dimension Versus Crack Depth for Fatigue Cracks..... in Ferritic Steel (Ekström and Wåle 1995)	3.7
Figure 3.8	Crack Opening Dimension Versus Crack Depth for IGSCCs in..... Austenitic Stainless Steel (Ekström and Wåle 1995)	3.8
Figure 4.1	Cracking in Reactor Pressure Vessel Cladding as Imaged by a DIAKONT Closed Circuit Video System (Vasiliev et al. 1999)	4.3
Figure 4.2	Axial PWSCC Crack in V.C. Summer Nuclear Station Pressure..... Vessel Nozzle to Pipe Weld.	4.4
Figure 4.3	Crud lines on the surface of the piece strongly resemble cracks and can hide real indications.	4.5
Figure 4.4	Visual Acuity Loss During Scanning. Left: a screen capture from..... when the camera is not moving.	4.5
Figure 4.5	Four images from Visual Inspections of Pressure Vessels and Piping.....	4.6
Figure 4.6	Resolution Demonstration with 25- μm (0.001-in.) Diameter Wire..... Image Taken using 1-megapixel Camera	4.8

Figure 4.7	12- μm (0.0005-in) COD Thermal Fatigue Crack on Machined Surface.	4.9
Figure 4.8	12- μm (0.0005-in.) Thermal Fatigue Crack on Smooth Surface.....	4.9
Figure 4.9	125- μm (0.005-in) COD and a 25- μm (0.001-in.) COD Mechanical..... Fatigue Crack on Smooth Surfaces.	4.10
Figure 4.10	Crack Detectability Versus Crack Opening Dimension (Enkvist J. 2002)...	4.11
Figure 5.1	Example of Current Performance Demonstration Standard Showing..... two 12 μm (0.0005 in.) Crossed Wires Against an 18% Grey Card	5.2
Figure 5.2	Jaeger Reading Chart with 25 μm (0.001 in.) Diameter Wire Stretched Below the Card Title.	5.3
Figure 5.3	Micrographs of 25- μm (0.001 in.) Wire and Crack with a 25 μm (0.001 in.) COD	5.4
Figure 5.4	Differences in Appearances of Cracks and Wires when Lit from..... the Side	5.4
Figure 5.5	Effects of Lighting Angle on 25- μm Wire and 125- μm Mechanical..... Fatigue Crack	5.5
Figure 5.6	1951 USAF Resolution Target Imaged by CaZoom(tm) PTZ System.....	5.7

Executive Summary

PNNL researchers conducted a study of the capabilities of visual testing as it relates to finding cracks in nuclear components in lieu of volumetric examinations using techniques such as ultrasonic testing currently required by the *ASME Boiler and Pressure Vessel Code Section XI Appendix VIII*. It is not clear, however, if this substitution can be made and maintain the same level of crack detection reliability. This report describes remote visual testing, performance demonstration standards for camera systems, the sizes of service induced cracks in reactor components, and an assessment of the reliability of camera systems at finding these cracks.

Current guidelines for testing visual systems use two crossed 12 μm (0.0005 in.) wires as a performance demonstration standard. If the system can detect the wires, it is supposedly sufficient to detect cracks and other flaws. In relation to current standards, some improvements are recommended. Line detection is not a reliable standard, and does not provide the level of accuracy that a combination resolution target test and a reading chart test can provide.

The average sizes of service-induced cracks in nuclear components were examined as part of this study. The crack opening dimension (COD) of service-induced cracks in nuclear components is one of the most important parameters affecting the reliability of visual tests. The CODs of thermal fatigue, mechanical fatigue and stress corrosion cracks were compiled from the literature and summarized in this report. Researchers in Sweden documented that in austenitic stainless steel, one can expect mechanical fatigue cracks to range from 5 to 250 μm (0.0002 to 0.001 in.) wide at the crack opening, with a median COD of 17.5 μm (0.0007 in.). Service-produced thermal fatigue cracks were found to range from 5 to 380 μm (0.0002 to 0.015 in.) wide, with a median COD of 27.5 μm (0.001 in.). Wåle and Ekström also characterized stress corrosion cracks in austenitic stainless steels. These cracks ranged from 5 to 107 μm (0.0002 to 0.004 in.) with a median size of 30 μm (0.001 in.). A large project by D.E. MacDonald examined 169 intergranular stress corrosion cracks and found CODs ranging from 5 to 310 μm (0.0002 to 0.012 in.) with a median COD of 40 μm (0.002 in.).

It has also been observed that COD is strongly related to surrounding stresses in the case of mechanical and thermal fatigue cracks. Stress corrosion cracks are more complex, and the COD is related to the susceptibility of the material to SCC, the surrounding stresses, and the history of the crack. The COD is not, however, strongly related to the crack depth into the material.

The results of this study on the reliability of visual testing systems related to average CODs show that the systems may not be able to reliably detect a significant number (often over 50%) of service induced cracks in nuclear components. To deal with the low probability of detection for many cracks, a parametric study should be performed to examine the relationship between the magnification and resolution of a camera system and the ability of the system to image very tight cracks in nuclear components. To determine the effectiveness of the remote visual testing being performed in the field, the findings also suggest a round-robin test to assess the procedures, equipment, and personnel employed in the field.

Foreword

Federal regulations require that nuclear power plants meet the design, operation, and inspection requirements of the American Society of Mechanical Engineers (ASME) Boiler and Pressure Vessel Code (B&PV). Section XI of the ASME B&PV Code provides the specific requirements for inspecting the systems, structures, and components; Section V of the ASME Code provides requirements for inspection methods, including volumetric (e.g., ultrasonic testing), surface (e.g., eddy current testing), and visual testing (VT).

Visual testing is conducted successfully for a variety of purposes, for example (1) to detect discontinuities and imperfections on the surface of components, (2) to detect evidence of leakage from pressure-retaining components, and (3) to determine the general mechanical and structural condition of components and their supports for conditions such as loose or missing parts. VT is performed directly or remotely using mirrors, telescopes, boroscopes, fiber optics, or cameras. While useful for many conditions, VT is primarily a surface examination and cannot provide information about what is under the surface. For example, VT cannot gauge the depth of a crack even though it is visible at the surface.

Unlike VT, volumetric examinations such as ultrasonic testing are able to detect and measure the depth and length of a crack in a material. This information is used as input to an analysis to determine if the crack must be repaired, in accordance with ASME Code provisions. Recently the U.S. nuclear industry has requested that the ASME and the NRC consider replacing volumetric and surface examinations of certain safety-related components with a VT method because of reduced radiation exposure to inspection personnel and reduced examination times with VT. The research documented in this report evaluates the capabilities of remote visual testing systems for detecting the types and sizes of cracking of interest. The research also evaluates the adequacy of current ASME Code requirements, suggests improvements to ASME Code requirements, and proposes additional work to determine the effectiveness of visual tests.

The results from the visual testing reliability assessment showed limitations for remote cameras in certain situations such as identifying very tight cracks in plant components. For effective crack detection, cameras must be held stationary over a location for a brief period of time because detection reliability is poor when the camera systems are “scanned” over an area. Further, the current resolution test is not sufficient for camera systems and should be replaced with more standard resolution and visual acuity tests.

Further experimental work is described to determine appropriate visual acuity parameters to ensure reliable detection of tight cracks under realistic conditions. Visual testing systems and personnel may need to qualify under performance demonstration requirements to ensure adequate inspection reliability. Upon completion of this additional experimental work, the NRC will have an adequate technical basis to assess the nuclear industry request to use a visual testing method in lieu of volumetric and surface examinations.

/RA/
Carl Paperiello, Director
Office of Nuclear Regulatory Research
U.S. Nuclear Regulatory Commission

Acknowledgments

The authors would like to thank members of the staff at the Pacific Northwest National Laboratory for their assistance in this work. Significant contributions were made by George Schuster, Charles Batishko, and Marino Morra. The authors would also like to thank the NRC for supporting this work and specifically, Deborah Jackson and Jim Davis for program guidance and support. The authors would also like to thank the South Texas Project for allowing the use of images and Everest VIT for demonstrating the CaZoom PZT camera system.

Thanks also go to Andrea Currie for editing this work and Earline Prickett for assistance in getting this report into the final format.

Abbreviations

ASME	American Society for Mechanical Engineers
BWRVIP	Boiling Water Reactor Vessel and Internals Project
COD	Crack Opening Dimension
DC	Definite Crack
DNC	Definite No Crack
EDM	Electrical Discharge Machining
EPRI	Electric Power Research Institute
ET	Electromagnetic Testing (Eddy Current)
FCP	False Call Probability
IGSCC	Intergranular Stress Corrosion Crack
ISI	Inservice Inspection
MTF	Modulation Transfer Function
NDE	Nondestructive Evaluation
NRC	Nuclear Regulatory Commission
PC	Probable Crack
PNC	Probable No Crack
PNNL	Pacific Northwest National Laboratory
POD	Probability of Detection
SCC	Stress Corrosion Crack
SKI	Swedish Nuclear Power Inspectorate (Statens Kärnkraftinspektion)
USAF	United States Air Force
UT	Ultrasonic Testing
VT	Visual Testing
VVER	Russian Designated Pressurized Water Reactor

1 INTRODUCTION

Since 2002, the U.S. Nuclear Regulatory Commission (NRC), Office of Nuclear Regulatory Research has funded a multiyear program, JCN Y6604, at the Pacific Northwest National Laboratory (PNNL) to evaluate the reliability and accuracy of nondestructive evaluation (NDE) techniques employed for inservice inspection (ISI). Through this program PNNL researchers provide technical bases and improved ISI programs for important reactor systems and components, evaluate the impact of ISI reliability on reactor system integrity, provide recommendations to the American Society of Mechanical Engineers (ASME) Code to improve the effectiveness and adequacy of ISI methods and programs, and provide technical assistance on NDE and related issues to the NRC program offices on an as-needed basis. The ASME Boiler and Pressure Vessel Section XI Code requires ISI to be conducted using both volumetric and surface techniques, depending upon access conditions and potential failure modes.

Recently, the U.S. nuclear industry proposed replacing current volumetric and/or surface examinations of certain components in commercial nuclear power plants, as required by the ASME Boiler and Pressure Vessel Code Section XI, with a simpler visual testing (VT) method. This expanded use of VT may be desirable, as these tests generally involve much less radiation exposure and examination times than do volumetric examinations such as ultrasonic testing (UT). However, for industry to justify supplanting volumetric methods with VT, an analysis of pertinent issues is needed to support the reliability of VT in determining the structural integrity of reactor components.

This report presents many of the issues involved with the reliability of VT. In Section 2 the VT technique is defined, and the limits of vision and factors that influence the reliability of a visual test are explored. The morphology of service-induced cracks typically found in nuclear power plant components is described in Section 3, followed by a discussion in Section 4 of the current state of the art in nuclear VT. Section 5 is a synthesis of key points presented in Sections 2 through 4 as they relate to the reliability of the visual testing technique within the nuclear power plant environment. Conclusions and recommendations are presented and discussed in Sections 6 and 7, respectively.

2 THE VISUAL TESTING TECHNIQUE

The technique of VT is deceptively complex. In its most basic terms, which can be summarized as “look at the test subject and try to detect a flaw,” VT does appear rather simple. However, when the size of a flaw is close to the resolution limit of the equipment used in the test (where *equipment* includes such things as the human eye or a video camera), the examinations become complex. Factors influencing the reliability of VT include, but are not limited to, light levels, lighting angles, surface conditions, the resolution limits of the equipment used, magnification, the contrast between the flaw and the surface, the amount of time spent examining the sample, and a host of human factors (Allgair et al. 1993, Moore et al. 2001).

A human eye with 20/20 vision is able to resolve features as small as $75\ \mu\text{m}$ (0.003 in.) in size at a distance of 25 cm (10 in.) (Allgair et al. 1993). This limit is based on the density of rods in the retina of the eye and on the diffraction limit imposed by the size of the eye. The eye is, however, able to detect features too small to be accurately resolve. It is possible under perfect conditions to detect a crack with a crack opening dimension (COD) as small as $10\ \mu\text{m}$ (0.0005 in.) on a mirror-polished surface (Michael Allgair et al,1993). The minimum detectable COD becomes much larger if the surface is rough or not perfectly clean. These limits do not account for factors such as scratches, machining marks, and any camouflaging effects offered by a macroscopic feature such as a weld root. Human factors play a large role in the test as well.

Any system used in VT (ranging from the naked eye to a digital closed-circuit TV system) will have a measurable visual acuity. The visual acuity of a system has four psuedo-independent measures (De Petris and Macro, 2000);

- a. visible minimum - the smallest dot the system can detect
- b. separable minimum (resolution) - the smallest separation between two lines the system can detect
- c. visual acuity by vernier - the ability to perceive spatial variation between two objects
- d. readable minimum (recognition capability) - the ability to recognize complex shapes such as letters or numbers.

These visual acuity parameters describe what a system can detect and discern. A system with a detection limit of $10\ \mu\text{m}$ (0.0004 in.) and a resolution limit of $30\ \mu\text{m}$ (0.0012 in.) at a given distance can “see” a $10\text{-}\mu\text{m}$ line on a sheet of paper but cannot resolve a $10\ \mu\text{m}$ gap between two $10\text{-}\mu\text{m}$ lines. A letter or number will appear to be a dot if it is larger than the visible minimum of a system, but below the readable minimum of the system. The letter will be identifiable only when it is above the recognition capability of the system.

The image sharpness produced by mechanical visual systems such as still and video cameras can be described in terms of their modulation transfer function (MTF). The MTF is a measure of the detected versus the actual contrast ratio as a function of the spatial frequency of the indications.

For example, a camera will generally show nearly 100% contrast on two black lines on a white background when the lines are far apart (low spatial frequency); however, if the lines are very close together (high spatial frequency), the system can blur the lines and the spaces between the lines together, reducing the contrast and thus reducing the MTF. Measuring the MTF of a system as a function of spatial frequency is a very reproducible and objective way to measure the visual sharpness of a camera system.

A resolution test is another common technique used to characterize the visual acuity of a system. A resolution test determines the smallest distance between two lines that can be discerned by the system. A resolution target generally has several sets of parallel or converging lines with notations on how many lines per millimeter are present at each point. Performing a resolution test consists of making an image of a standard resolution target and determining the point at which the system can no longer separate the lines. The main problem with resolution tests is that they rely on the observer to determine which lines are separable and which are not, adding an element of subjectivity to this measurement. However, a resolution test has the advantage of being faster and easier to administer than a test of system MTF. Examples of commercially available resolution targets include the Institute of Electrical and Electronics Engineers (IEEE) Resolution Target, which conforms to the standard STD 208-1995, "*Measurement of Resolution of Camera Systems*", the 1951 U.S. Air Force Resolving Power Target, and the International Organization for Standardization (ISO) Camera Resolution Chart. The details of which targets conform to which standard can be found in Sine Patterns L.L.C. 2004.

The maximum possible visual acuity of a video or digital system can be described by comparing the native resolution of the system to the size of the area on which the system is focused. This measure of visual acuity assumes perfect optics and a perfect electronic capture of the image. Using this method, a 1 megapixel (1200 x 800 pixels) camera that can focus on an area 75 mm x 50 mm (3 in. x 2 in.) would have a pixel size of 0.0625 mm/pixel. Any indications that fall below this size would be pixelated and recorded as a lower-contrast shadow in the larger pixel, as the contrast from the indication is averaged with the background in the pixel. The color and shading of the pixel is dependent on the contrast between the indication and the background and on the MTF of the camera. An example of a linear indication in which the width of the line is significantly less than the pixel size is shown in Figure 2.1.

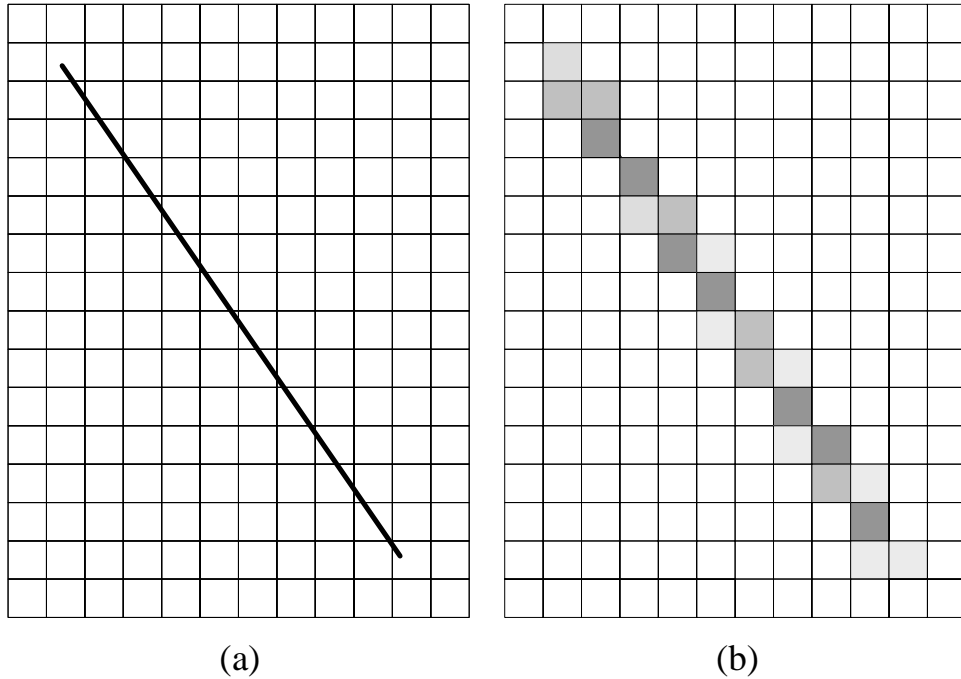


Figure 2.1 Pixelation of line (a) into lower-contrast image (b).

A common, although not very reliable, technique used in the nuclear industry as a performance standard for visual systems is to determine if a given system can detect very small diameter wires or thin printed lines. Although using line detection to test a camera system has a long history, it is not well respected by many experts in visual testing as exemplified by this excerpt from Allgair et al. (1993):

Because simple line detection is a relatively gross task, it can be a poor performance standard, allowing detection of a highly blurred image. This does not emulate sharpness quality recognition for evaluation of weld discontinuities. A 750 μm (30 mil) black line can be reliably detected by individuals classified as legally blind (20/200 corrected both eyes). The 750 μm (30 mil) and the even smaller 25 μm (1 mil) widths should not be used as performance standards because they do not determine image sharpness. While this technique is relatively quick and simple to perform, it only measures the “visible minimum” for long linear indications and does not measure a system’s resolution or recognition limits. If the wire or printed line has a strong enough contrast against the background a linear feature well below the resolution of a system can be detected.

Another important variable in visual acuity is the speed at which the visual system scans over the inspected area. The term *kinetic vision acuity* is used for the visual acuity of a given system

when scanning a moving target. The loss of visual acuity as a function of scan speed is highly dependent on the technology used to capture the images. A high-speed film camera can capture sharp images of a bullet in flight, while a poor video system can show noticeable blur at slow scan speeds. In general, high-quality image capture with video systems requires that the camera be halted over the area to be inspected for at least 2 or 3 seconds.

Two important parameters used to quantify how well an indication can be identified from an image are the size of the indication on the image and the signal-to-noise ratio. The size of the indication is best described in this context as the number of resolution lines. A historical rule of thumb from aerial reconnaissance photography is that three resolution lines on a side are needed for detection; five resolution lines along a side are needed for identification (Jensen, 1968). However, these rules were developed for round objects and are difficult to apply to crack detection, as cracks are very long (many resolution lines with a typical system) relative to their width (possibly less than one resolution line with the best of systems). The signal-to-noise ratio is determined by comparing the signal from the contrast between the crack opening and the base metal to the noise from machining marks, cleaning marks, and other extraneous indications on or near the flaw.

3 SERVICE-RELATED CRACKING IN NUCLEAR REACTOR COMPONENTS

Cracks in stainless steel components, especially near welds, are the flaws that are of most interest in volumetric, surface, and visual testing of reactor components and piping. Components in nuclear reactors are subjected to a wide variety of stresses and chemical environments, which could lead to several forms of cracking. It is important to understand the morphologies of these cracks and how difficult they are to detect.

Section 3.1 addresses the causes and surface appearance of mechanical fatigue, thermal fatigue, and stress corrosion cracks. This information was gathered from the literature and from archived cracked samples examined at PNNL. A literature search on the factors that influence the COD for different types of cracks is documented in Section 3.2.

Section 3.3 presents data from the Swedish Nuclear Power Inspectorate (SKI) on the CODs for several types of fatigue and stress corrosion cracks in stainless steels. The SKI report (Ekström and Wåle 1995) is a compilation of data from several studies on the subject of crack sizes. The data include crack width and give the mean, median, and distribution of COD for several types of cracks.

3.1 Surface Appearance of Common Cracks

To understand the ability of VT to detect various cracks in reactor components, it is important to understand the different types of cracks and their surface-breaking properties. Common cracks in reactor components include mechanical fatigue cracks, thermal fatigue cracks, and stress corrosion cracks. Each type of crack is formed differently, and each has a different surface morphology.

Mechanical fatigue cracks are formed when a material is subjected to repeated stress cycles. Cracks formed in this way are relatively straight and typically do not branch significantly, if at all. The COD is highly dependent on the stresses in the material. The crack is widest during the phase when the tensile stresses perpendicular to the crack face are at their highest. When the stresses that form the crack are not present, the COD shrinks considerably and may close almost entirely. Often there is not much corrosion inside the crack. A typical mechanical fatigue crack is shown in Figure 3.1.



Figure 3.1 25- μm (0.001-in.) COD Mechanical Fatigue Crack in Stainless Steel

Thermal fatigue cracks can be manifested in regions of components with stratified hot and cold water levels that change with time. Thermal fatigue cracks will typically form in patterns. In a material without any predominant directional stresses, thermal fatigue cracks often form in a fabric-like or cobblestone pattern in the affected material. If the material in question is under a tensile stress, then multiple small thermal fatigue cracks often form with the cracks perpendicular to the direction of the stress. There may or may not be oxidation inside the crack, and thermal fatigue cracks can have a very small COD. The COD of a thermal fatigue crack is strongly dependent on the stresses perpendicular to the crack opening. A pair of thermal fatigue cracks that formed near one another is shown in Figure 3.2. Note the variation in linearity and the background noise due to machining operations.

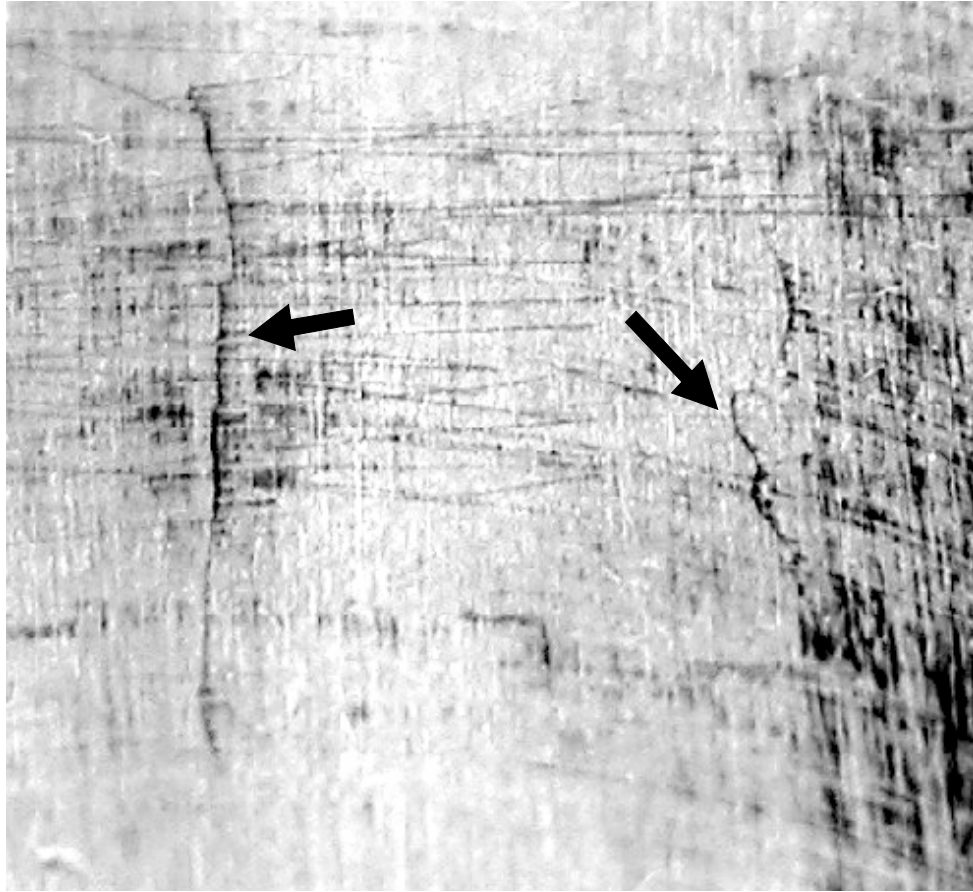


Figure 3.2 Two 15- μm (0.0005-in.) COD Thermal Fatigue Cracks on Machined Stainless Steel Surface. There is discoloration and chipping at the crack opening, increasing the visibility of the cracks. (Image converted to black and white and contrast-enhanced).

Stress corrosion cracking (SCC) is caused by a combination of stress, a sensitized material, and a corrosive environment. In stainless steel, these cracks usually form along heat-affected zones near welds, as the welding process causes the heat-affected zone to become sensitized. These cracks vary in appearance, ranging from a single crack to a series of cracks lying together in a slightly feathered pattern but nearly always following the sensitized zone. Welds also have internal residual stresses created in the welding process, which provide the stress needed to propagate a SCC. Older SCCs may have some oxidation on their inside surfaces causing grains of material to dislodge from the crack face, widening the SCC. However many SCCs have a very small COD. An SCC following the heat-affected zone in a weld is shown in Figure 3.3. Note the liquid penetrant residue from a previous surface examination to enhance crack detection.

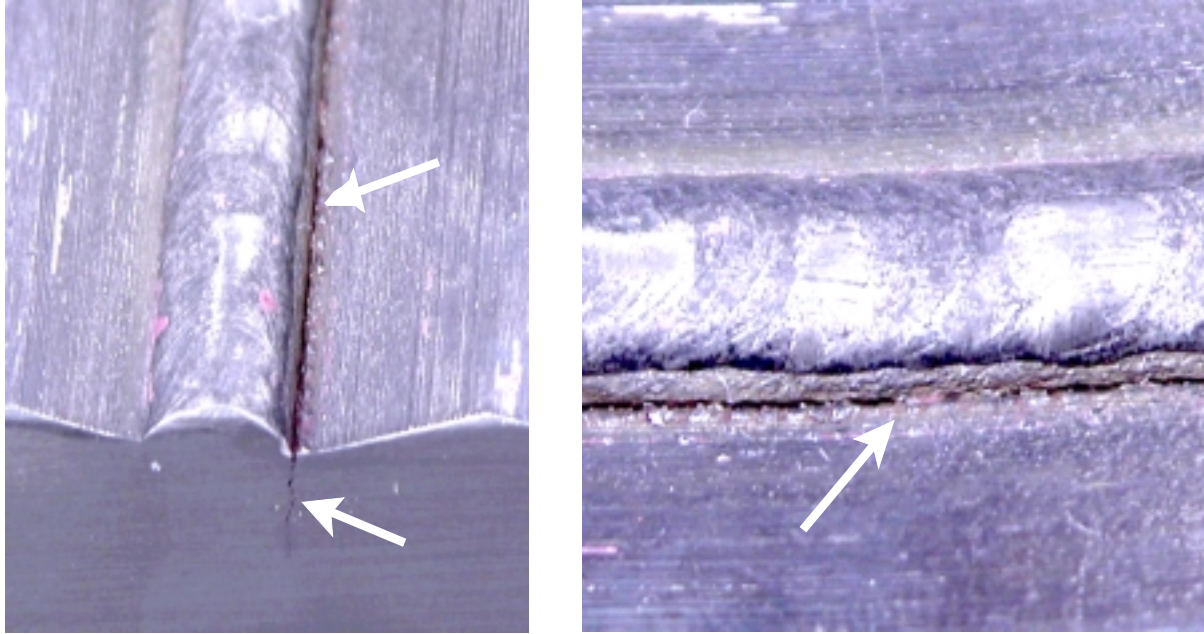


Figure 3.3 Two Views of 125- μm (0.005-in.) COD Stress Corrosion Crack along Weld in Stainless Steel.

Although there are several types of stress corrosion cracking, most of the data that has been collected at PNNL and from the literature is related to intergranular stress corrosion cracking (IGSCC). IGSCC is one of the more common forms of SCC in nuclear reactor components and is a reasonable analog for other types of SCC. Thus, the IGSCC results can be considered relevant for most SCC issues. Primary water stress corrosion cracking (PWSCC) can occur within the weld, which can complicate detection.

3.2 Factors influencing Crack Opening Dimension

For thermal and mechanical fatigue cracks, the largest factor governing the crack opening dimension is the stress acting perpendicular to the crack opening (Yoneyama et al. 2000, Kim et al. 2002; Xaio et al 2002). According to the Westergaard stress function, the maximum COD is given by

$$COD = \frac{4a\sigma}{E} \quad (3.1)$$

(Chen, D.L. et al. 1996) where a is the crack depth, σ is the stress on the material, and E is Young's modulus. In a fatigue crack, the COD strongly depends on the state of the material when the crack is measured. If a mechanical fatigue crack is examined when the material is not in tension, the crack can be closed entirely. Without a stress σ , the theoretical COD is zero. Often, the only stress available to hold a fatigue crack open is the residual stress causing the crack formation or resulting from fabrication processes. As the residual and other stresses at a given point are not generally known, one cannot use the COD to predict the through-wall depth of a crack.

It is worth noting that nuclear reactor components are examined during outages when systems are not at operating temperature and pressure. Some of the main sources of stress are not present when the components are examined. With all of the pressure relieved and the differential temperatures across components eliminated when the reactor is shut down, the COD of the cracks in the reactor will most likely decrease to a minimum size.

The factors influencing the CODs for stress corrosion cracks are more complex than for fatigue cracks. Stress corrosion cracks form because of an interaction between a sensitized material, a corrosive environment, and stress in the material. When SCC occurs, the opening size may depend on the susceptibility of the material and the residual stresses around the crack. A stress corrosion crack can have a very small COD if one grain boundary is affected in a lightly susceptible material or a very large COD in a very susceptible material when several surface grains are dislodged from the crack (Garcia et al. 2001). A highly sensitized material can form many SCCs in the same area, which may then link up and form a crack with a large COD. A less sensitized region will have fewer and tighter SCCs. There is no reliable way to gage the depth of an SCC based on its COD. Examples of SCCs with small and large CODs are shown in Figure 3.4. It is worth noting that both cracks have penetrated to essentially the same depth.

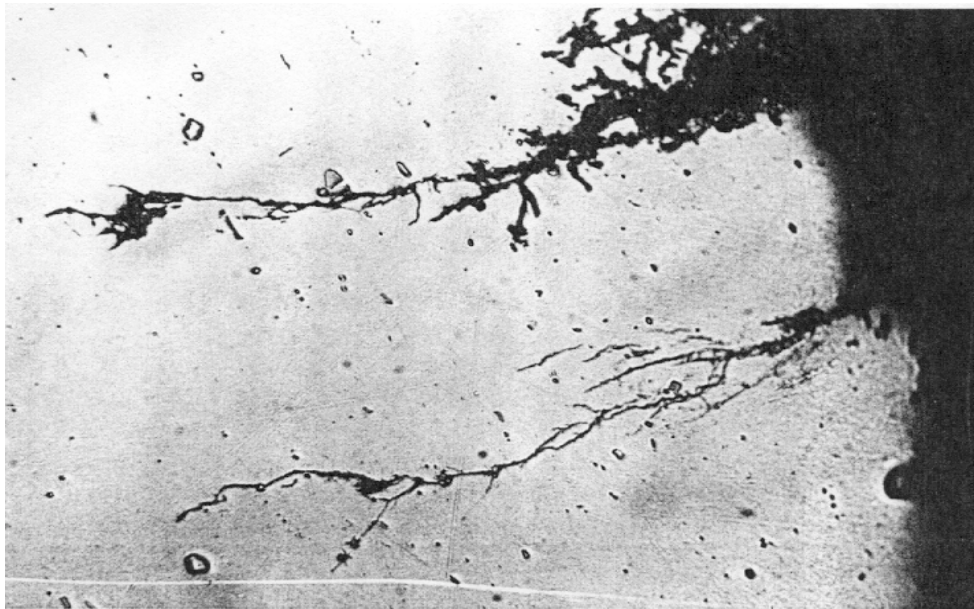


Figure 3.4 Two Stress Corrosion Cracks in Locking Bolt (100X magnification) (Morrin et al. 1978)

3.3 Compiled Crack Opening Dimensions for Cracks in Austenitic Stainless Steel

Several hundred cracks of various types in many materials have been characterized and documented in the literature in the United States and Europe. The results show that COD is

highly variable over all crack types and materials. The findings also show that COD is largely independent of the crack depth.

Swedish researchers (Ekström and Wåle 1995) reported that in austenitic stainless steel, mechanical fatigue cracks (seven cracks were evaluated) can be expected to range from 5 to 250 μm (0.0002 to 0.010 in.) wide at the crack opening, with a median COD of 17.5 μm (0.0007 in.). The twenty service-produced thermal fatigue cracks evaluated were found to range from 5 to 380 μm (0.0002 in. to 0.015 in.) wide, with a median COD of 27.5 μm (0.0011 in.). Ekström and Wåle also characterized stress corrosion cracks in austenitic stainless steels. These cracks ranged from 5 to 107 μm (0.0002 to 0.004 in.) with a median COD of 30 μm (0.0013 in.). A project by D.E. MacDonald (MacDonald 1985) examined 169 IGSCC's and found CODs ranging from 5 to 310 μm (0.0002 in. to 0.012 in.) with a median COD of 40 μm (0.0016 in.). The works by Lapides and Stenefjall are referenced in the SKI document.

Figures 3.5 and 3.6 contain charts that show a compilation of work done by several groups who have characterized the CODs of fatigue cracks and SCCs. The middle line in each bar represents the median crack size, and the upper and lower dashed lines represent the sizes of the 75% and 25% limits. Figures 3.7 and 3.8 show the distributions of CODs to crack through-wall depth.

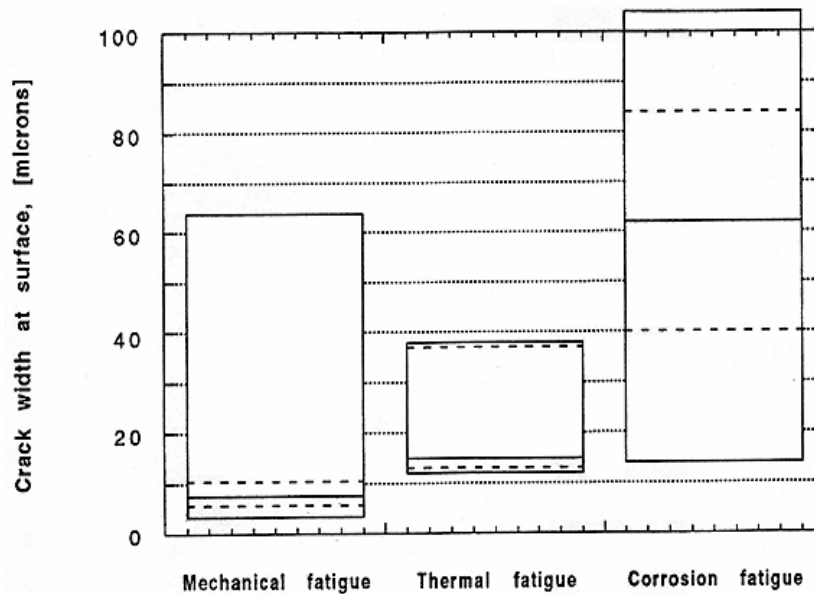


Figure 3.5 Crack Opening Dimension Distribution for Fatigue Cracks (Ekström and Wåle 1995)

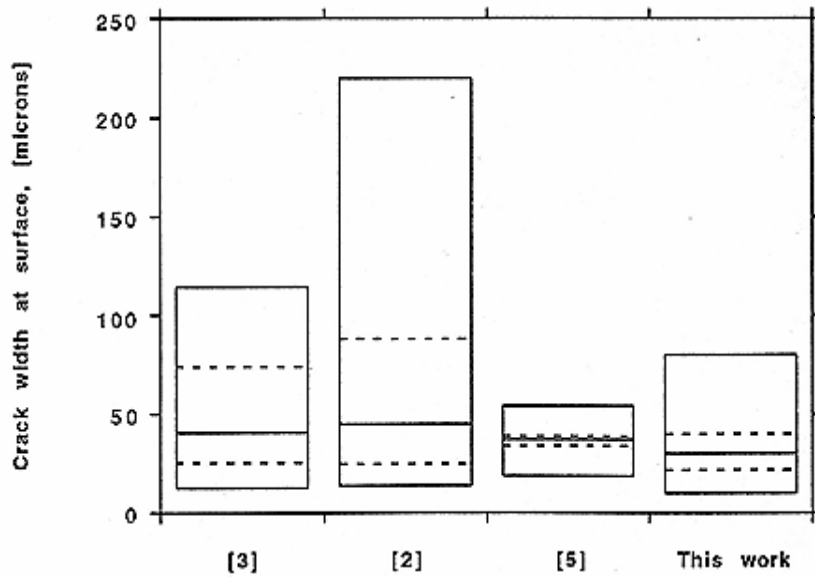


Figure 3.6 Crack Opening Dimension Distribution for Stress Corrosion Cracks. Study 3 was conducted by MacDonald, 2 by Lapides, 5 by Stenefjall, and “This work” refers to the work of Ekström and Wåle (1995).

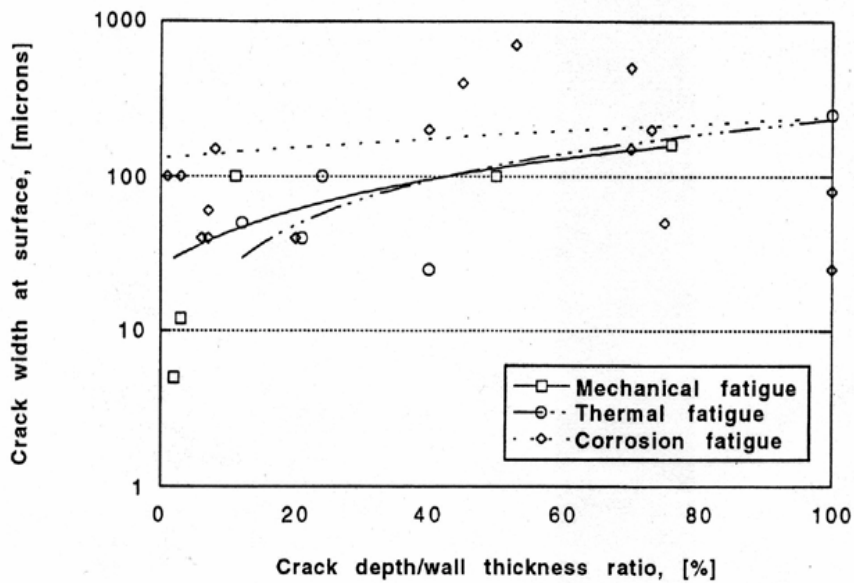


Figure 3.7 Crack Opening Dimension Versus Crack Depth for Fatigue Cracks in Ferritic Steel (Ekström and Wåle 1995)

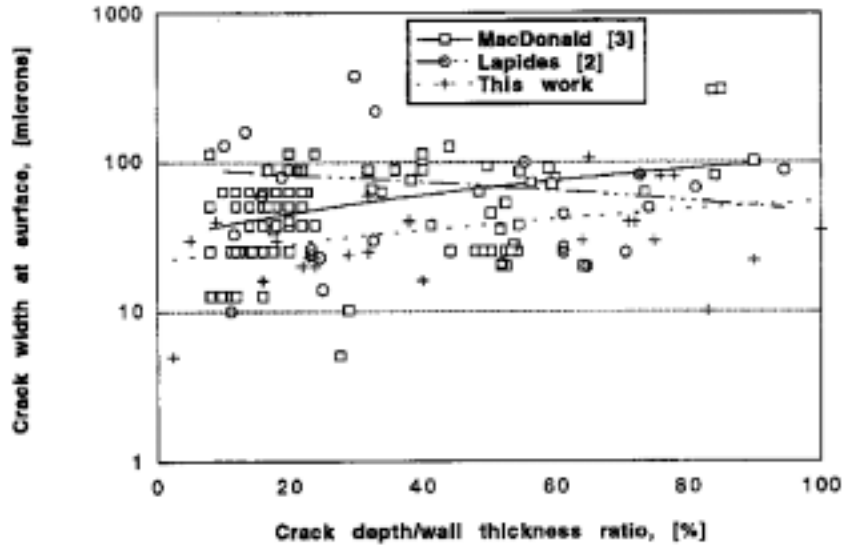


Figure 3.8 Crack Opening Dimension Versus Crack Depth for IGSCCs in Austenitic Stainless Steel (Ekström and Wåle 1995)

Figures 3.5 and 3.6 show that cracks in reactor components have a wide distribution of CODs with a significant number of cracks having a COD below $12 \mu\text{m}$ (0.0005 in.). Figures 3.7 and 3.8 further reinforce the premise that there is a weak relationship between the COD of a crack and its through-wall penetration.

4 REMOTE VISUAL TESTING IN THE NUCLEAR INDUSTRY

As piping and other components in a nuclear power station are generally underwater and in high radiation fields, they need to be examined from a distance with radiation-hardened video systems. Remote visual testing has been used by nuclear utilities to find cracks in pressure vessel cladding in pressurized water reactors (PWRs), core shrouds in boiling water reactors (BWRs), and to investigate leaks in piping and reactor components. These visual tests are performed using a wide variety of procedures and equipment.

The types of cameras used in remote visual testing of nuclear reactor components and the Electric Power Research institute (EPRI) guidelines for VT-1 examinations (visual examinations meant to find cracks and similar flaws) are described in Section 4.1. The guidelines are discussed in terms of what is known about visual acuity parameters, as described in Section 2.

In Section 4.2 examples of images from actual visual tests in nuclear reactors are presented. These examples were taken from a technical article on nondestructive testing in the Russian nuclear industry (Vasiliev et al. 1999) and from videotapes provided by the NRC; they cover several nuclear reactors. The images show some of the capabilities of visual testing and some problems, such as motion blur and cleaning issues, that can adversely affect visual tests in the field. Additional illustrations are provided in Appendix A.

The ability of visual tests, using both human eyes and video systems, to detect cracks based on their COD is discussed in Section 4.3. The visibility of cracks in archived samples at PNNL is described and photographs of wires and selected cracks are shown, and their relevance to the camera's ability to image the cracks is discussed. Finally, the results of a literature search on visual tests and their abilities to detect cracks are presented.

4.1 Overview

The techniques for remote visual testing use high-resolution video cameras to examine reactor components and welds. Camera systems used for remote visual inspections include, among other systems, the DIAKONT™ Reactor Pressure Vessel TV inspection system and the Everest VIT Ca-Zoom PTZ™ system. These systems have video resolutions ranging from 470 to 600 vertical lines on the screen. They are typically able to zoom to magnifications on the order of X10 to X25. Their advertised specifications are given in Appendix B. It is notable that the DIAKONT™ camera system advertises to be accurate to detect features of 40 μm or larger.

Utilities today follow the EPRI guidelines for VT-1 tests on nuclear components (BWR Vessel and Internals Project-3 1995). These guidelines specify that the examined surface must be clean and for underwater testing that the water be clean and clear. The VT-1 guidelines also specify which areas around a weld should be examined, how to measure the sizes of indications found, and how to test the resolving power of the visual equipment used for the test. The EPRI guidelines use two 12- μm (0.0005-in.) wires or notches as a resolution calibration standard.

Unlike UT and electromagnetic testing (ET) sections of the guidelines, the VT technique demonstration uses no actual cracks when testing the ability of the cameras to detect and characterize cracks. The results of the technique demonstration for VT from a nonproprietary section of BWRVIP-03 (1995) pages 4-31 and 4-32 are reproduced below:

It is expected that variations in crack tightness will affect the capability of the visual method to determine the actual length of the cracking. Experiments have been made at the NDE center on camera resolution using 0.0005-inch diameter stainless steel wires. These cameras were lowered into a 20-foot deep water-filled tank. Various lighting intensities, camera angles, and camera-to-object distances were evaluated. The 0.0005-inch wires were placed on the white background of the tank, on a stainless steel mockup shroud, and on a rusted section of carbon steel. Each of the wires was detectable with each of the cameras utilized. The wire on the painted surface was easily detected at about 16 inches with each camera system. The wire on the stainless steel shroud mockup was difficult to detect and required much manipulation of the camera before the wire was seen. The wire on the rusty section of the carbon steel was easily detected by reflection of the light from the external lights on the cameras. This particular detection was related to the light reflection and not to contrast. Care must be taken to ensure that the detection of the 0.0005-inch diameter wire is essentially representative of detection of a crack of the same width.

According to the EPRI guidelines (BWRVIP-03 1995), the camera systems employed were marginally able to detect the 0.0005-inch (12- μm) diameter wire on a steel background. Thus, the camera systems had difficulty passing a detection test which is a poor measure of system resolution capabilities. Additionally, it is the understanding of the authors that the length-sizing tests performed by EPRI used 3-mm (1/8-in.) wide black strips of tape and did not test the ability of the remote VT systems to size real cracks. This technique demonstration leaves many unanswered questions as to the ability of the subject VT systems to detect cracks with narrow CODs in field conditions. The differences between detection of wires and cracks will be addressed in more detail in Section 5 of this report.

4.2 Examples of Remote Visual Tests

Remote visual tests have been performed routinely on reactors to examine core shrouds and other components. Some examples are provided.

The results of a remote visual examination on the interior of the Russian Kalininskaja VVER reactor pressure vessel using a DIAKONT reactor TV inspection system are shown in Figure 4.1 (Vasilev V. G. et al 1999). The cracks are in the cladding of the pressure vessel and have CODs of between 50 to 200 μm (0.002 to 0.008 in).



Figure 4.1 Cracking in Reactor Pressure Vessel Cladding as Imaged by a DIAKONT Closed Circuit Video System (Vasiliev et al. 1999)

One crack imaged using VT was a through-wall axial crack in the piping of V.C. Summer Nuclear Station. The crack was detected by indirect means; specifically, boric acid deposited from primary coolant leaking through the pipe was the first indication of a crack. The pipe was visually examined twice. The first examination used a video camera on the end of a long pole; the second used a robotic scanner. The first VT test missed the crack, while the second, performed by WesDyne, successfully detected the crack. The contrast and size of the crack image was enhanced as there was corrosion of the ferritic steel of the pressure vessel nozzle forging which bled back through the crack, lining it with reddish corrosion products. The crack is shown in Figure 4.2.

PNNL obtained copies of videotapes of VT exams conducted in U.S. nuclear power plants from the NRC. The taped visual inspections show the conditions under which visual tests are conducted and the appearance of the surfaces being inspected.



Figure 4.2 Axial PWSCC Crack in V.C. Summer Nuclear Station Pressure Vessel Nozzle to Pipe Weld. The COD of the crack is not known.

An examination of the videotaped images shows that the level and method of cleaning of the component can strongly influence the results. While it has been previously noted that any extraneous material on the surface of a component being examined with VT may mask a relevant feature on the surface, improper cleaning can result in crud lines (streaks of dirt left over from cleaning) and rub marks that can also look like cracks. The part or region to be examined needs to be cleaned of all dirt and crud while not leaving the remnants of the cleaning process. An example of a component with observable crud lines is shown in Figure 4.3.

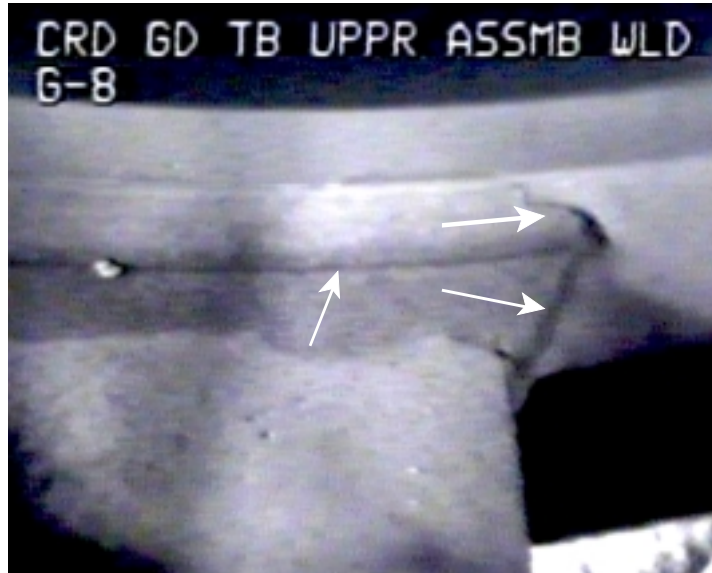


Figure 4.3 Crud lines on the surface of the piece strongly resemble cracks and can hide real indications.

An example of the loss of visual acuity when a camera is scanning is shown in Figure 4.4. The picture is significantly sharper when the camera is stationary (system normal visual acuity) over a zone as opposed to scanning (system kinetic visual acuity). This lower kinetic visual acuity demonstrates that a system capable of passing a resolution test when not moving can possibly fail when the camera is being scanned.



Figure 4.4 Reduction of Visual Acuity During Scanning. Left: a screen capture from when the camera is not moving. The vertical lines are sharp and the picture is relatively clear. Right: a screen capture of different area when the camera is moving. The vertical lines are blurred, as is the rest of the picture.

The videotapes provided important insights on the interior condition of pipes and cladding in

U.S. reactor pressure vessels (RPVs). The interiors of the RPVs have machining and grinding marks over most surfaces. Some areas are discolored and possibly slightly oxidized. These scratches and machining marks provide a lot of visual “noise” that may mask cracking. Four examples of the interior conditions of pressure vessel internals and piping are shown in Figure 4.5.

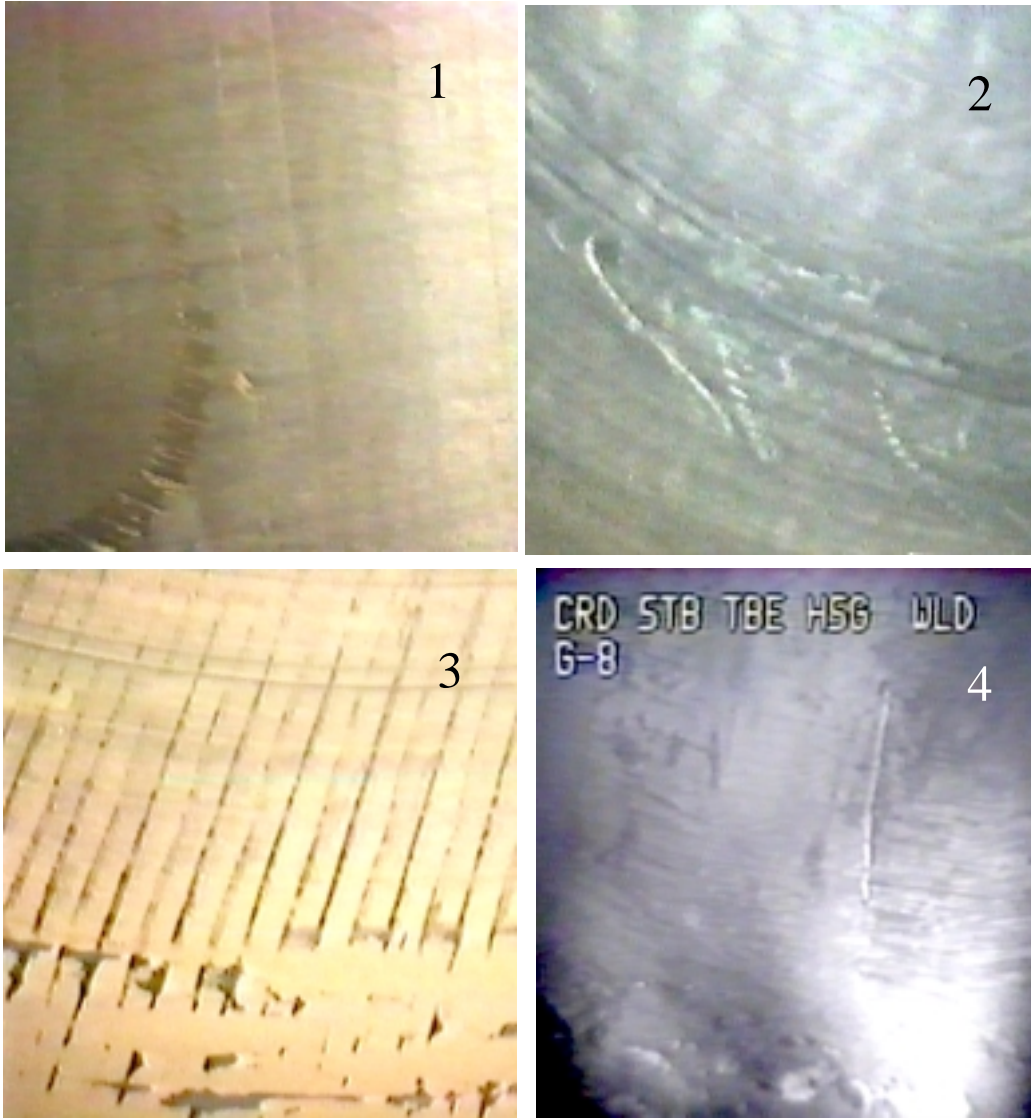


Figure 4.5 Four Images from Visual Inspections of Pressure Vessels and Piping. 1. Close-up of the metal near a weld showing scratches and markings. 2. Close-up of a pipe interior showing scratches and marks. 3. Manufacturing axial and circumferential markings on the interior of a PWR pipe. 4. Scratches and a vertical rubbing mark on a control-rod drive stub tube housing.

4.3 Probability of Crack Detection Vs. Crack Opening Dimension

To date, no comprehensive studies of the probability of various video systems used for remote visual testing to detect cracks relative to their COD have been published. Work on samples present at PNNL provides useful insights into crack detection capabilities, and limited published work enhances our understanding.

Pacific Northwest National Laboratory has a variety of cracked specimens available for study. Most specimens contain mechanical fatigue cracks, with a smaller number of thermal fatigue cracks and IGSCC samples. Various specimens were examined, some with unaided VT and with an optical micrometer to determine CODs and visibility of the cracks. Several of the IGSCC samples were cut, and the COD was measured from the side. The results of these measurements are given below in Table 4.1.

Table 4.1: Crack Information on the PNNL Cracked Specimens						
Sample ID	Crack No.	COD (μm)	Depth	Length (cm)	Type	Visibility Level ^(a)
4	1	25	unknown	3.2	Mech fatigue	3
	2	25	unknown	13	Mech fatigue	4
	3	12	unknown	2.5	Mech fatigue	4
	4	12	unknown	1.3	Mech fatigue	4
	5	12	unknown	1.3	Mech fatigue	3
3	1	25	50%	1.9	Mech fatigue	3
	2	125	75%	5.7	Mech fatigue	1
	3	25	50%	4.4	Mech fatigue	3
	4	25	30%	1.3	Mech fatigue	4
A139	1	12	50%	1.3	Mech fatigue	1
9150	1	12-25	50%	1.3	Mech fatigue	1
b117	1	12	50%	1.9	Thermal Fatigue	5
b118	1	12	60%	2.5	Thermal Fatigue	2
d32a	1	125	30%	3.2	IGSCC	2
b217G	1	25	na	na	IGSCC	na
b217B	1	12	na	na	IGSCC	na
B214	1	12	na	na	IGSCC	na
B213	1	25	na	na	IGSCC	na
D107	1	12	na	na	IGSCC	na

^a The visibility levels are defined as follows:

- 1 The crack can be seen clearly from any angle
- 2 The crack is visible from all angles with close inspection
- 3 The crack is easy to find with inspection but not visible from all angles
- 4 The crack is difficult to find and only visible from a few angles
- 5 The crack is nearly impossible to see and is only visible from one specific angle
- na Visibility assessments were not possible in the destructively-examined IGSCC samples

The mechanical fatigue cracks that have been examined show a poor relationship between crack depth and COD and crack length. The extreme cases were two 50% through-wall cracks, one with a COD of 125 μm (0.005 in.) and a length of more than 5 cm (2 in.), and a crack with a COD of 12 μm (0.0005 in.) and a length of 1 cm (0.4 in.). These contrast with a 25% through-wall IGSCC crack with a COD of 125 μm (0.005 in.). All cracks had a similar shape and morphology. All were relatively straight and did not branch significantly on the surface.

Figure 4.6 shows that a 1-megapixel, 3X zoom digital camera used to study crack openings can easily image a 25- μm (0.001-in.) Diameter wire. Photographs of selected cracks are shown in Figures 4.7 through 4.9. These photos were taken under laboratory conditions, using a tripod and careful lighting. Figure 4.7 shows a thermal fatigue crack with a COD of 12 μm (0.0005 in.). This thermal fatigue crack is not difficult to image, as it has some discoloration around the crack opening that has turned black and contrasts strongly with the steel. This crack has propagated 50% through-wall. Figure 4.8 shows a thermal fatigue crack that also has a COD of 12 μm (0.0005 in.). The material has been sanded down to a smooth surface, making the crack difficult to detect from most angles. It is also difficult to photograph clearly, as the crack is shown as a barely perceptible line. This crack also has a 50% through-wall depth. Figure 4.9 shows an 80% through-wall mechanical fatigue crack with a COD of 125 μm (0.005 in.) and a 50% through-wall mechanical fatigue crack with a COD of 25 μm (0.001 in.) on a smooth surface. The 80% through-wall crack is very easy to detect from nearly any angle. The 50% crack can be seen only on close inspection. As some of the cracks are on the edge of the camera detection ability, printouts and photocopies of these pages may not show all of the details even though the contrast had been digitally enhanced

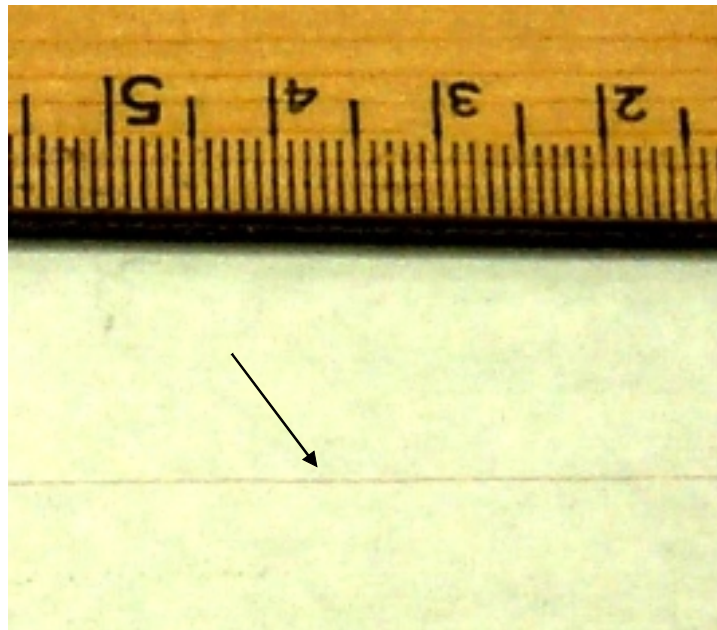


Figure 4.6 Resolution Demonstration with 25- μm (0.001-in.) Diameter Wire Image Taken using 1-megapixel Camera

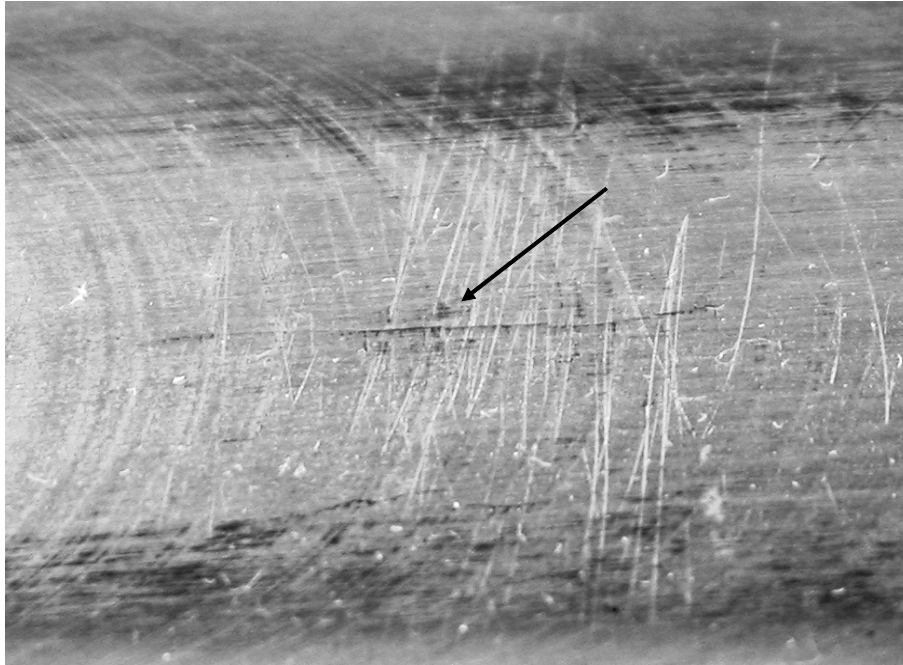


Figure 4.7 12- μm (0.0005-in) COD Thermal Fatigue Crack on Machined Surface. The crack is clearly visible despite its small COD, as there is discoloration around the crack opening



Figure 4.8 12- μm (0.0005-in.) Thermal Fatigue Crack on Smooth Surface

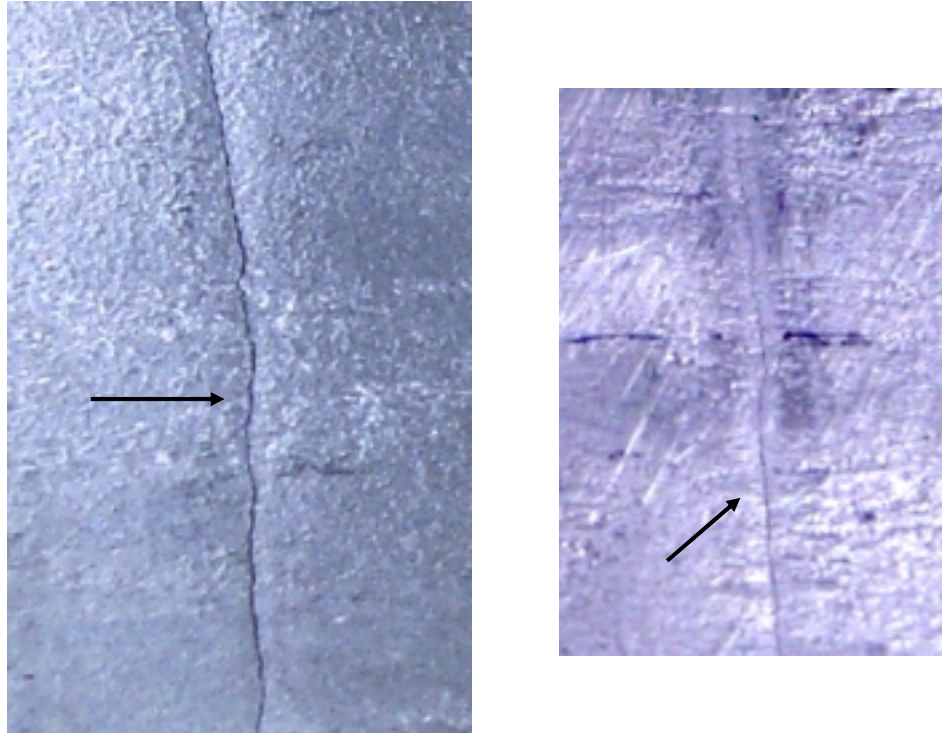


Figure 4.9 125- μm (0.005-in) COD and a 25- μm (0.001-in.) COD Mechanical Fatigue Crack on Smooth Surfaces. The 125- μm COD crack is clearly visible, while the 25- μm COD crack is visible only on close inspection.

The photography of the cracks demonstrates that a digital camera able to detect a 25- μm (0.001-in.) wire may not be able to resolve similarly-sized cracks. In several cases a very close visual inspection could find cracks that were invisible to the digital camera. During the direct visual inspections we were able to examine the specimens at a much shorter distance than with the digital camera, allowing for better detection.

A human factors study performed in Sweden (Enkvist 2003) contains useful information on the evaluation of visual testing. A series of cracked ceramic specimens, molded to have the surface appearance of the region near a weld, was examined underwater by ten operators using a high resolution 752 x 582 pixel video camera with an 18X optical zoom and with lighting provided by with two 15-W halogen lamps. Only one viewing angle and a single distance of 200 mm (7.87 in.) from the test samples were used. The tests were therefore somewhat more restrictive than an actual field test. The area inspected by the system at maximum magnification was 47 x 35 mm (1.8 in. x 1.4 in.) with a resulting pixel size of 60 μm (0.0024 in.). This study is therefore considered to be a conservative estimate of the capabilities of remote visual testing. The operators were instructed to note all linear indications that could be detected and label them as Definite Cracks (DC), Probable Cracks (PC), Probable No Cracks (PNC), and Definite No Cracks (DNC). Detection and false call rates were then evaluated under “Strict” guidelines counting only DCs as hits, “Normal” counting both DCs and PCs as hits, and “Lenient” which

counted all but DNCs as hits. The results are shown in Figure 4.10. Cracks above 40 μm COD were easily detected, while cracks below 20 μm COD had, at best, a 20% probability of detection using the “Lenient” grading scale.

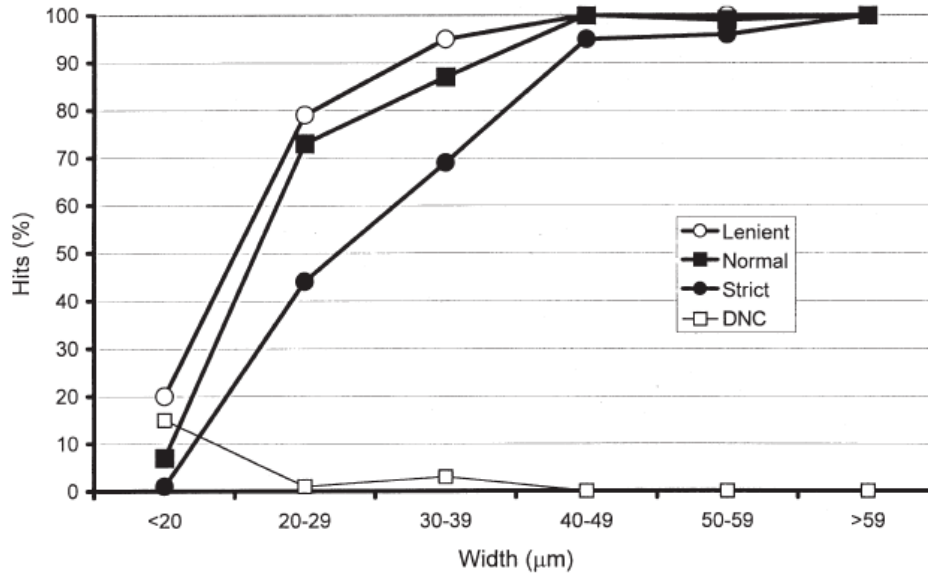


Figure 4.10 Crack Detectability Versus Crack Opening Dimension (Enkvist J. 2002)

Work has been conducted in Germany on visually testing reactor components (D’Annucci 2001). The results reported the technique is able to resolve indications as small as 7 μm (0.0003 in.) in size, but only with a system capable of applying a dye in order to enhance visual performance (a penetrant test typically cannot be performed underwater). A more standard visual system was used in Sweden to test reactor components, and the reported detectable limit for defects was 20 μm (0.0008 in.) (Efsing et al. 2001).

5 DISCUSSION

Some of the points mentioned previously are examined in more detail in this section. First, the crack opening dimension is discussed in terms of how it relates, or does not relate, to crack depth. Second, the current resolution test used to calibrate visual testing equipment in the nuclear industry is described in terms of its abilities to discern visual acuity parameters, and how well this resolution test can determine if a camera system can detect tight cracks. The use of a resolution pattern is then proposed as a better system to determine the visual acuity of a camera system. Another important parameter in visual testing, the scanning technique used to cover the area of interest, is discussed. Finally, a brief comparison of ultrasonic testing and visual testing is made.

5.1 Crack Opening Dimensions

The crack sizes measured at PNNL match the Swedish work in showing that thermal fatigue cracks have a wide variability in COD. This variability in COD versus length and depth probably accounts for the limited level of literature relating these parameters. Essentially, the COD of a crack does not provide any meaningful information as to how far through-wall the crack has propagated.

The COD is a function of several variables. Important factors include, but are not limited to, the material hardness, the applied load, the crack length, residual stresses around the crack opening, and the degree of corrosive attack at the crack opening. Which specific variables are important depends on the type of crack involved. In the mechanically fatigued PNNL samples, several cracks with very different CODs were found within a few inches of each other. The literature reports that the width of an IGSCC is fairly random and is a factor of how many grain boundaries at the crack opening are affected.

A very important point to note is that tighter SCC and fatigue CODs may fall below what is visible on even a well-polished metal surface. Virtually all fatigue cracks and 75% of the IGSCCs have a COD smaller than $75\ \mu\text{m}$ (0.003 in.), the resolution limit for 20/20 vision. Given the number of machine and fabrication marks on the interior surfaces of piping and cladding in a reactor pressure vessel, a VT system requires at least 20/20 vision, if not significantly better, to distinguish true cracks from these surface features.

5.2 Resolution and Acuity Standards for VT Equipment

The standard used to calibrate a camera system during visual tests is a very important check of the ability of the system to detect cracks. A good standard can demonstrate that the system has resolution capability to detect the features in question and that examined areas are lighted from the most advantageous angles. There are, however, several problems with the current standard test used for camera systems to perform remote VT. The current standard target, which consists of two crossed $12\text{-}\mu\text{m}$ (0.0005-in.)-diameter wires is not, in reality, a resolution test, but a

detectable minimum test. The wires can be well below the resolution capability of the system and still be detected if there is high contrast between the wire and background. If service-induced cracks on reactor components appeared as high-contrast lines on smooth, clean, polished surfaces in the absence of any visual noise such as machining marks or welding marks, the standard wire test might be sufficient. Under realistic test conditions in nuclear reactor components a camera system could pass this test and still miss cracks significantly larger than 12 μm (0.0005 in.) COD.

An example of a camera system using a 12- μm (0.0005-in.) wire detection test is shown in Figure 5.1. It should be noted that the resolution target also contained a series of letters for use as a reading chart. For ease of viewing and printing, contrast in the Figure 5.1 has been digitally enhanced. The wires are detectable as low-contrast fuzzy linear indications against the 18% neutral grey card. The video camera used in this example has a pixel size of 7.5 pixels/mm (190 pixels/in.) or 125 μm (0.005 in.), this being measured in a different frame which included an image of a ruler. The 12- μm wire is one tenth of the width of each of the pixels and is well below the resolution of the system at this magnification. Had the contrast between the wire and the background been weaker, or if any visual noise were near the wires, the wires would probably not be detectable.

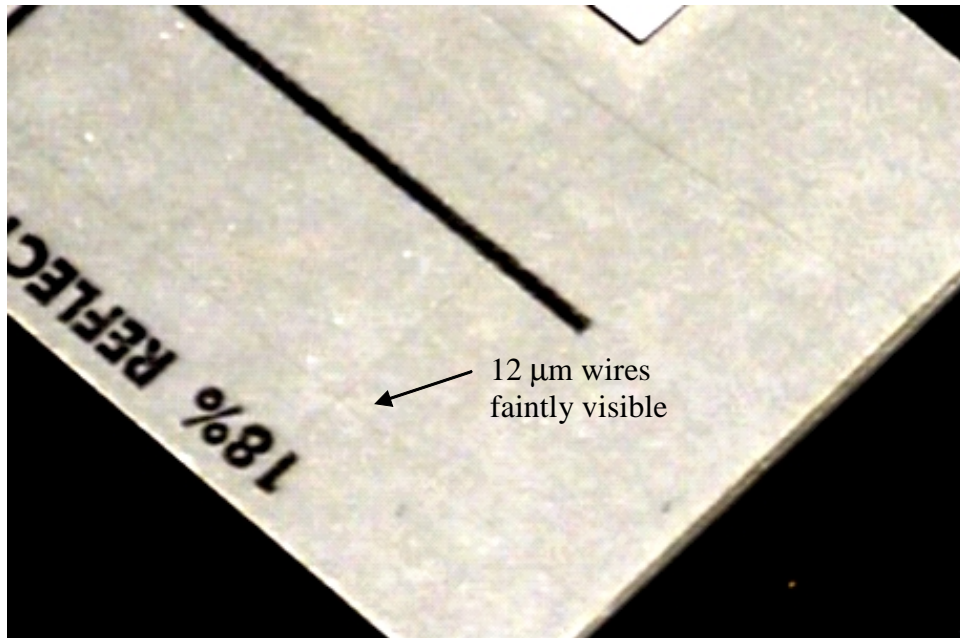


Figure 5.1 Example of Current Performance Demonstration Standard Showing two 12 μm (0.0005 in.) Crossed Wires Against an 18% Neutral Grey Card

Simple line detection using thin wires also fails when trying to characterize the readable minimum (recognition capability) acuity of a system. As shown in Figure 5.2, a 25 μm (0.001 in.) diameter wire is visible as a low-contrast line against a white Jeager reading card while the

smallest writing that is easily readable on the card corresponds to 20/60 vision. An intentionally out-of-focus photograph of the same chart is presented in Appendix A.

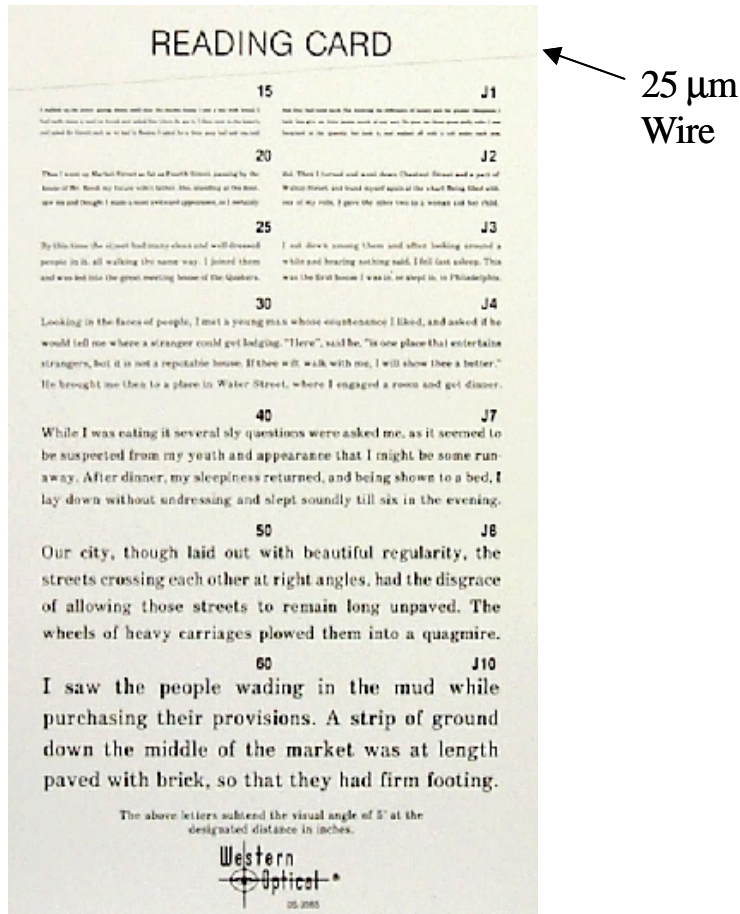


Figure 5.2 Jaeger Reading Chart with 25 μm (0.001 in.) Diameter Wire Stretched Below the Card Title.

In addition to the issues related to testing the camera resolution, the wire standard is also problematic on the issue of illumination angle. There are important differences between visually detecting a stretched wire and detecting a crack. A wire sitting on the surface of a piece has a very different geometry than does an inset crack, and a wire has a very different response to light than does a crack. Lighting angles that make a wire very visible may not be effective for crack detection. One difference between a wire and a crack is that a round wire surface is very good at reflecting light, while cracks do not produce strong reflections and often are detectable only as a dark line. Another issue is that a wire will cast a relatively long shadow when a light source is placed near the surface of the piece, while a crack can never look larger than it actually is, based on shadowing effects. Figures 5.3 through 5.5 show the differences between cracks and wires. Figure 5.3 shows the different appearance of a wire and crack of the same width. Figure 5.4 is a

schematic demonstrating how wires and cracks differ with side lighting. Figure 5.5 shows a 25- μm (0.001-in.) wire next to a 125- μm (0.005-in.) crack when lighted from the side and when lighted directly.

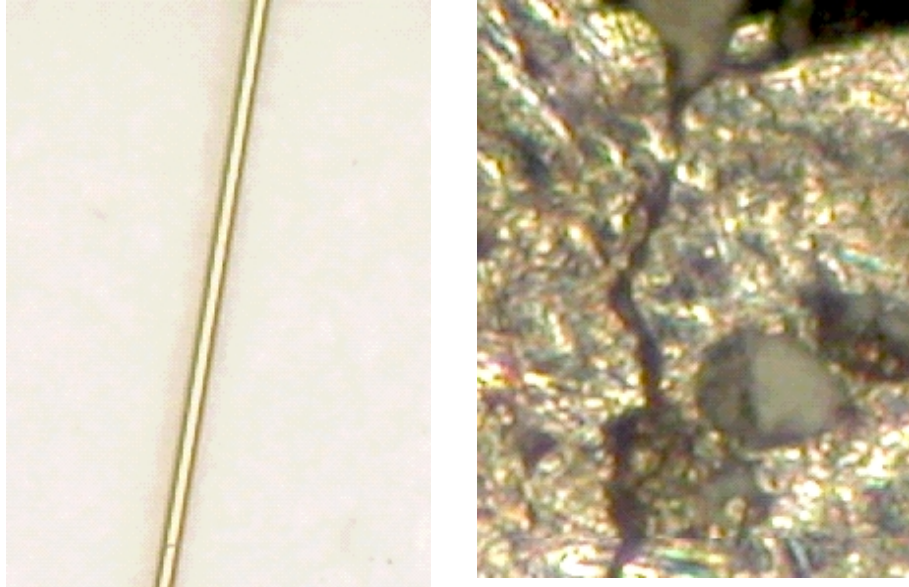


Figure 5.3 Micrographs of 25- μm (0.001 in.) Wire and Crack with a 25 μm (0.001 in.) COD

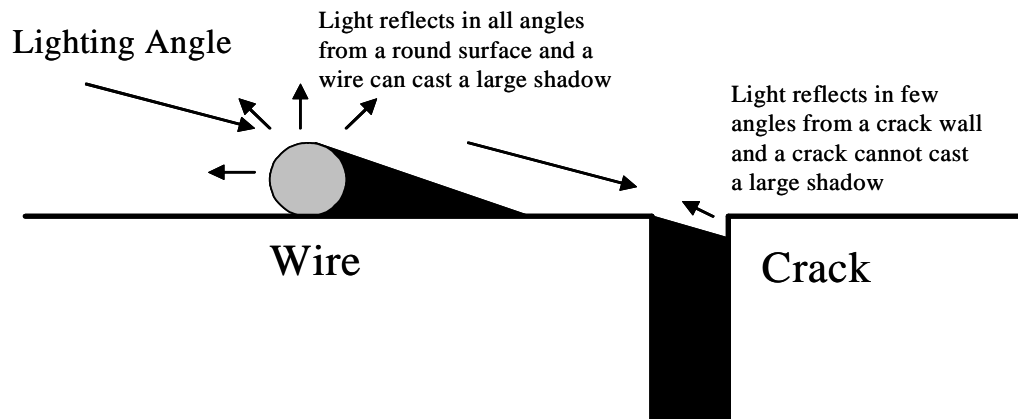
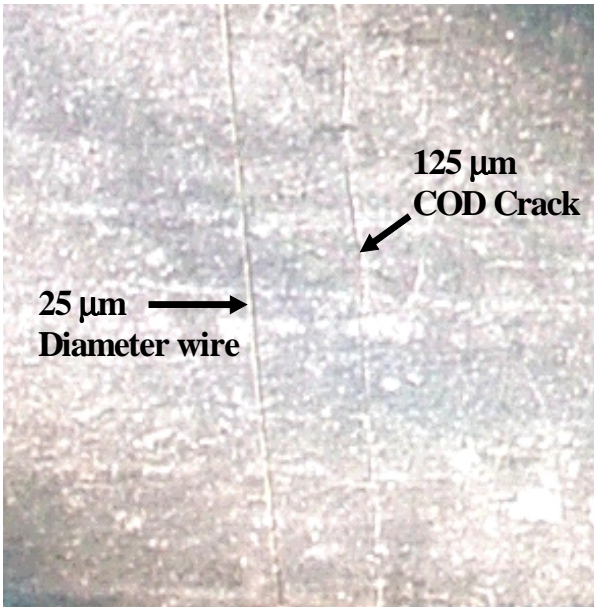


Figure 5.4 Differences in Appearances of Cracks and Wires when Lighted from the Side

Side Lighting



Direct Lighting

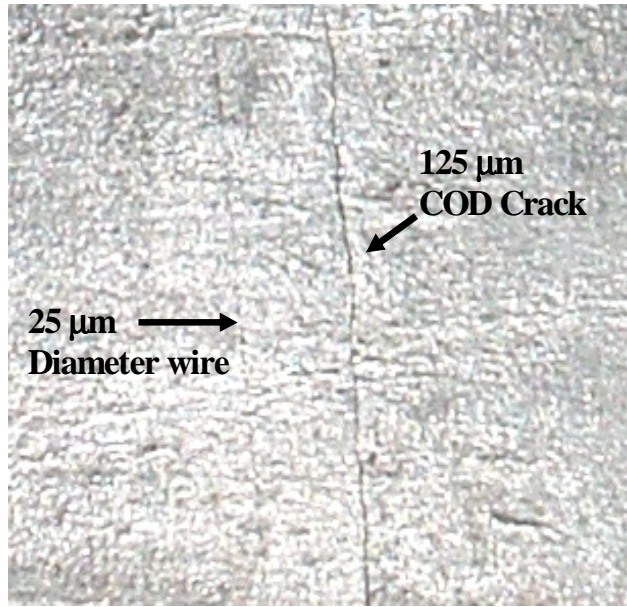


Figure 5.5 Effects of Lighting Angle on 25- μm Wire and 125- μm Mechanical Fatigue Crack

As Figure 5.5 shows, the side-lighted wire shows up much better than does the much larger crack. This effect is caused by a combination of the effects shown in Figure 5.4. Also interesting is that the crack also appears bright in places and dark in others, as the light is reflecting from some of the facets in the crack. When the specimen lighting is directly overhead, the crack and wire appear as dark lines, with the crack correctly appearing to be larger than the wire. As with the performance standard, a more representative standard for determining the optimum lighting could be a block with an EDM notch or crack with an appropriate width. The use of a notch or crack to arrange the lighting would provide far more accurate feedback as to which lighting setup is best for finding a crack.

A more accurate performance standard would be a cracked specimen with an appropriately sized crack and a representative surface finish and texture. The cracked surface would be a better test of camera and operator abilities to find and recognize a crack. It would also enable the operator to properly configure the illumination angles to allow for the highest possible contrast between the crack and the weld surface.

5.3 Resolution Testing and the Modulation Transfer Function

Measuring the MTF of a camera involves examining a sinusoidal pattern with a camera and analyzing the resulting image to measure the contrast ratio of the pattern as a function of spatial frequency. Testing the MTF is reasonably complex, however. Although testing the MTF of a system is more objective than a simple resolution test, for field applications a resolution test may be superior.

Several standard resolution tests are available to characterize optical systems and could be adapted to characterize visual testing systems in the field. These resolution tests would provide a much better measure of system acuity than the current simple line detection tests. These resolution tests could be applied in the same way as the current wire tests, that is, a resolution target would be tested before an examination to assure that the system is working properly. A standard resolution test can quickly and easily show the operator how many lines per millimeter are resolvable by the system.

An example of a resolution test is shown in Figure 5.6. This resolution test was conducted using a 1951 USAF Resolving Power Target. The highest resolution was measured under laboratory conditions in air at approximately 4 cm (1.6 in.) from the resolution target. Using this target, researchers determined the system resolution to be 11.31 line pairs per millimeter, meaning that the system could discern a gap as small as $44\ \mu\text{m}$ (0.0017 in.) between two black lines. The inspected area was 2 cm x 1.5 cm (0.78 in. x 0.59 in.) indicating there were 32 pixels/mm (812 pixels/in.) for a pixel size of $33\ \mu\text{m}$ (0.0013 in.). If this test had been performed in water (correcting for the refractive index of water as compared to air) the pixel size would have been $25\ \mu\text{m}$ (0.001 mil).

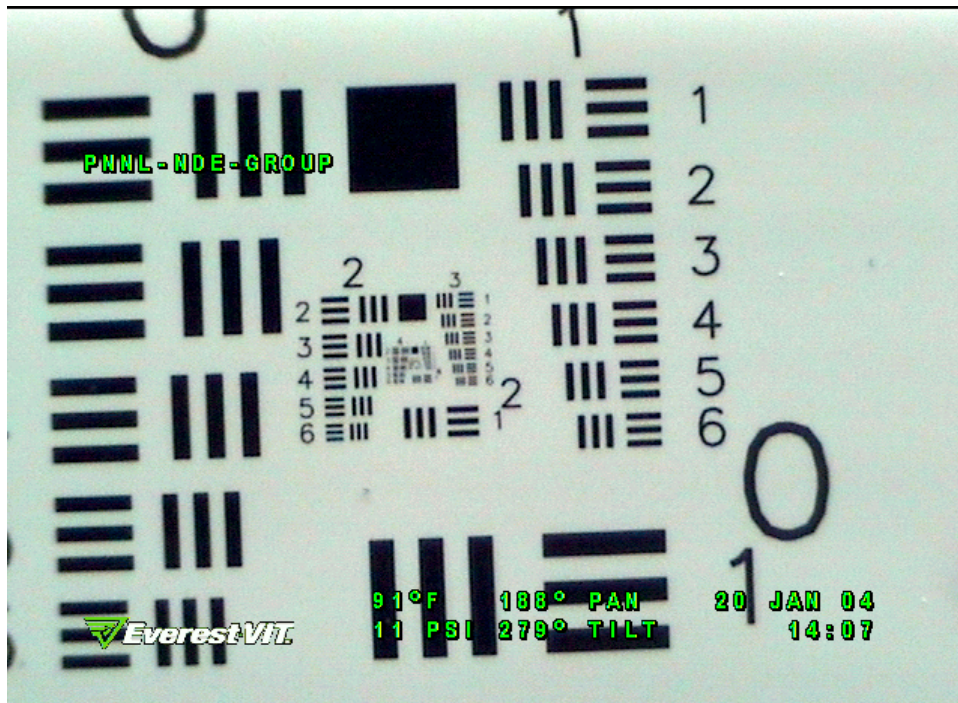


Figure 5.6 1951 USAF Resolution Target Imaged by CaZoom PTZ System

5.4 Scanning Technique

Because systems being used for remote visual examination lose acuity during scan motions, either this loss of visual acuity must be characterized or examinations of the components must be performed by moving the camera to a new position, holding the camera over the area for a few seconds, and then moving to the next area segment. Holding the camera over each area would also allow the human observer to carefully look over the area in question. Another possibility is to take resolution tests while the system is scanning over a resolution test target while the system is moving at the speed that would be used during scans.

A system with 640 x 480 pixels with sufficient magnification to achieve a pixel size of 10 μm (0.0004 in.) would have an inspection area of 6.4 mm x 4.8 mm (0.25 in x 0.19 in.) To scan a typical piping girth weld with an inside diameter of 61 cm (24 in.) and cover 25 mm (1 in.) on either side of the weld with a five-second hold over each point would require a scan time on the order of 5 hours. The scan times would be decreased with higher-resolution systems because the latter could cover larger areas while maintaining the same pixel size.

Systems capable of performing these scans will probably require automation to allow for precise indexing that would be needed to ensure coverage. A manually aimed system (i.e., a camera on the end of a pole and manipulated with ropes) would not be able to hold over an area or index reliably

over a few millimeters at a time.

5.5 A Comparison of Visual and Ultrasonic Testing

Ultrasonic testing and VT have many very important differences. Ultrasonic testing is a volumetric technique that is able to determine the presence of a crack and characterize the depth and length of a crack in the material. Visual testing is a surface test that cannot gage the depth of a crack and generally requires a subsequent ultrasonic test to determine the depth of any cracks detected. Both UT and VT can be subjective. The difficulties in ultrasonic tests include detecting features in materials that are acoustically attenuating and/or anisotropic. Discriminating between echoes caused by geometric or metallurgical features from echoes caused by cracks and other flaws can be very difficult at times. Difficulties in visual tests include detecting cracks with a small COD and discriminating between scratches, machining marks, and other surface imperfections. Ultrasonic tests are able to clearly detect and size cracks with very small CODs. If performed properly, visual tests may detect cracks in any material, including materials difficult to examine with ultrasound such as cast stainless steels. The task of discriminating between flaws and innocuous features is the job of the person or people analyzing the data. This adds an important variable, the skill of the examiner, to both tests.

The reliability of ultrasonic examinations has been carefully measured in several round-robin tests. These tests put the ultrasonic procedure, equipment, and personnel through a series of trials using a statistically significant number of flawed and unflawed samples. It is possible to measure the probability of detecting (POD) a crack and the false call probability (FCP) in which one claims an uncracked sample has a crack.

The reliability of VT is not understood well enough to compare it to ultrasonic studies. There is no literature available on round-robin type tests or for VT equipment and operators. There are no measurements of POD compared to FCP for VT testing to relate to the extensive database on ultrasonic round robin results and the results from performance demonstration tests conducted according to the ASME Code, Section XI (ASME 2001, Appendix VIII).

6 CONCLUSIONS

Based on the analysis documented in this report, the following conclusions can be drawn:

- ! Cracks with identical through-wall penetration can have very different CODs and surface lengths.
- ! Cracks with the same COD can have very different visibility levels depending on the surface features of the crack and the surface features of the cracked material.
- ! The current standard resolution target, two crossed 12- μm (0.0005-in.) wires, is not sufficient. A rigorous resolution test should include a reading chart and a resolution chart and possibly a tight EDM notch or an actual crack to determine optimum illumination angles.
- ! Although no comprehensive study on the reliability of visual testing has been performed, estimates can be made based on the technical specifications of the visual testing equipment, the field experience with this equipment, and studies by Enkvist (2003). The reliability of underwater crack detection appears to drop significantly when the cracks have a COD of less than 40 μm , and cracks with a COD of 20 μm or smaller do not appear to be reliably detectable with current remote visual testing technology and applied techniques.
- ! Although current visual testing techniques have been demonstrated to be able to detect wide cracks, more than half of the fatigue cracks and a quarter of the stress corrosion cracks in the Ekström and Wåle study (1995) have CODs of less than 20 μm (0.0008 in.). This small crack size relative to the reliably detected crack sizes suggest that current visual testing systems and techniques would probably miss a significant fraction of cracks in nuclear components.
- ! It is possible that with a visual testing system with a sufficiently high resolution and with enough magnification, taking a series of still photos (or scanning and stopping over each area) could check an area for very tight cracks with reasonable accuracy. Values for the resolution, magnification, and possible scan speeds for such an inspection are not currently known.
- ! Because systems lose visual acuity as the camera scans over a surface, the camera almost certainly needs to be held stationary when making critical images.

7 RECOMMENDATIONS

The current resolution calibration standard for VT systems (crossed 12- μm wires) in nuclear power plants is not sufficient to determine the visual acuity of a remote system. A calibration standard that uses a reading chart, a Vernier chart, and a resolution chart would provide much more confidence in accurately characterizing the visual system used in the examination. Also, lighting angles and intensities for crack detection need to be optimized for an inset target as opposed to any targets that sit above the surface. This issue could be addressed by using a laser cut notch, a tight EDM notch, or a test crack.

Further experimental work is suggested to determine the value for the visual acuity parameters (resolution, pixel size) to reliably detect very tight cracks under realistic conditions. A parametric study of crack detectability as a function of visual acuity parameters would be very useful in evaluating visual systems and methods used for visual testing.

The inspection reliability of the various VT systems, calibration standards, and procedures is not well characterized. A round-robin test of remote visual systems and techniques is needed to quantify the reliability, identify limitations, and provide a basis to recommend improvements to the VT process.

The relative effectiveness of VT as compared to ultrasonic testing and eddy current testing has not been well characterized. To ensure that visual tests are providing the same level of inspection reliability as the ultrasonic tests, VT systems and personnel may need to undergo performance demonstration. Performance demonstrations are required for ultrasonic personnel, procedures, and equipment, and any test that would be used to replace ultrasonic tests must be held to the same high standards.

8 REFERENCES

Allgair M.W., S. Ness, P. McIntire, and P.O. Moore. 1993. *Nondestructive Testing Handbook—Volume 8 – Visual and Optical Testing*. 2nd ed. American Society for Nondestructive Testing, Columbus, Ohio.

American Society of Mechanical Engineers. 2001. “Rules for Inservice Inspection of Nuclear Power Plant Components.” Section XI in *The 2001 ASME Boiler and Pressure Vessel Code*. ASME International, Washington, D.C.

BWR Vessel and Internals Project. 1995. *Reactor Pressure Vessel and Internals Examinations Guidelines*. BWRVIP-03, Electric Power Research Institute, Palo Alto, California.

Chen, D.L., Weiss, B., and Stickler, R. 1996. “A Model for Crack Closure” In *Engineering and Fracture Mechanics* Vol. 53 No. 4; 493-509

D’Annucci, F. 2001. “Latest Technologies and Results in Reactor Vessel Head Penetration Inspection.” In *Proceedings of the 3rd International Conference on NDE in Relation to Structural Integrity for Nuclear and Pressurized Components*. November 14–16. 2001, Seville, Spain. Tecnatom s.a., Seville.

De Petris C., and C. Macro. 2000. “Verification of the resolution capability for equipment used for visual testing.” In *Proceedings of the 15th World Congress on Non-Destructive Testing*. AIPnD — the Italian Society for Non-Destructive Testing and Monitoring Diagnostics, Brescia, Italy. Available at <http://www.ndt.net/article/wendt00/papers/idn300/idn300.htm>.

Efsing P., J.-Å. Berglund, C. Sandelin, and A. Werner. 2001. “Visual inspection of brackets for emergency core cooling system in Barsebäck Unit 2.” In *Proceedings of the 3rd International Conference on NDE in Relation to Structural Integrity for Nuclear and Pressurized Components*. November 14–16. 2001, Seville, Spain. Tecnatom s.a., Seville.

Ekström P., and J. Wåle. 1995. *Crack Characterization for In-Service Inspection Planning*. SKI Report 95:70, Swedish Nuclear Power Inspectorate, Stockholm, Sweden.

Enkvist J. 2003. “A study of operator performance in a visual NDT inspection task by remote video camera.” *Insight* 45(4):252-257.

García C., F. Martin, P. De Tiedra, J.A. Heredero, and M.L. Aparicio. 2001. “Effects of prior cold work and sensitization heat treatment on chloride stress corrosion cracking in type 304 stainless steels.” *Corrosion Science* 43(8):1591–1599.

Jensen N. 1968. *Optical and Photographic Reconnaissance Systems*. John Wiley & Sons, Inc., New York.

Kim Y.-J., N.-S. Huh, and Y.-J. Kim. 2002. "Reference stress based elastic-plastic fracture analysis for circumferential through-wall cracked pipes under combined tension and bending." *Engineering Fracture Mechanics* 69(3):367-388

MacDonald D.E. February 1985. *IGSCC Detection in BWR Piping Using the Miniatic*, EPRI Report NP-3828

Moore M., B. Phares, B. Graybeal, D. Rolander, and G. Washer. 2001. *Reliability of Visual Inspection for Highway Bridges — Volume I: Final Report*. FHWA-RD-01-020, NDE Validation Center, Office of Infrastructure Research and Development, Federal Highway Administration, McLean, Virginia.

Morin C.R., K.F. Packer, and J.E. Slater. 1978. "Failure analysis associated with mining and heavy equipment." In *Metallography in Failure Analysis: Proceedings of a Symposium on Metallography in Failure Analysis*. J.L. McCall and P.M. French, eds. Plenum Press, New York.

Sine Patterns. 2004. "Standard Charts." Sine Patterns L.L.C., Pittsford, New York. Available at <http://www.sinepatterns.com/Standards.htm>.

Vasiliev V.G., M.B. Bakirov, and M.V. Grigoriev. 1999. "Non-Destructive Inservice Inspection of the VVER Reactor Pressure Vessels in Russia." In *Proceedings of the First International Conference on NDE in Relation to Structural Integrity for Nuclear and Pressurized Components*. October 20-22, 1998, Amsterdam, Netherlands. Woodhead Publishing Limited, Cambridge, England.

Xaio Q.Z., and B.L. Karihaloo. 2002. "Approximate Green's functions for singular and higher order terms of an edge crack in a finite plate." *Engineering Fracture Mechanics* 69(8):959-981.

Yoneyama H., M. Senoo, J. Miharada, and N. Uesugi. 2000. "Comparison Test of Echo Heights Between Fatigue Crack and EDM Notch." In *Proceedings of the 2nd International Conference on NDE in Relation to Structural Integrity for Nuclear and Pressurized Components*. May 24-26, 2000, New Orleans, Louisiana. Electric Power Research Institute, Palo Alto, California.

APPENDIX A

Supplemental Photographs of Samples

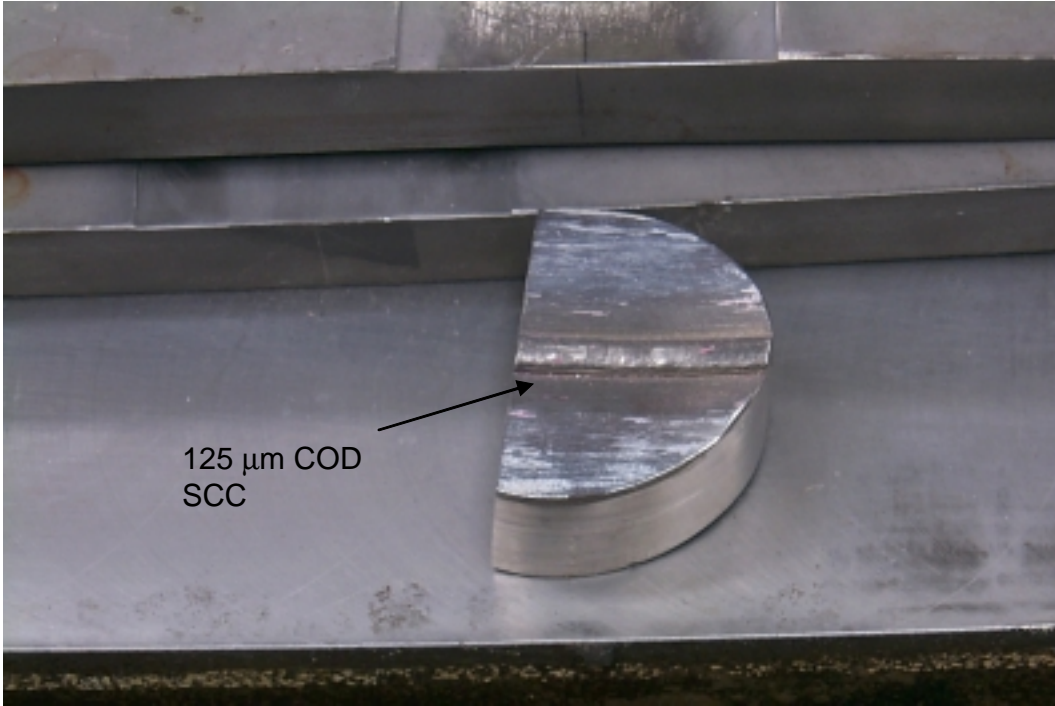


Figure A.1 Sample d32a with a 125- μm COD Stress Corrosion Crack Along the Weld Root.

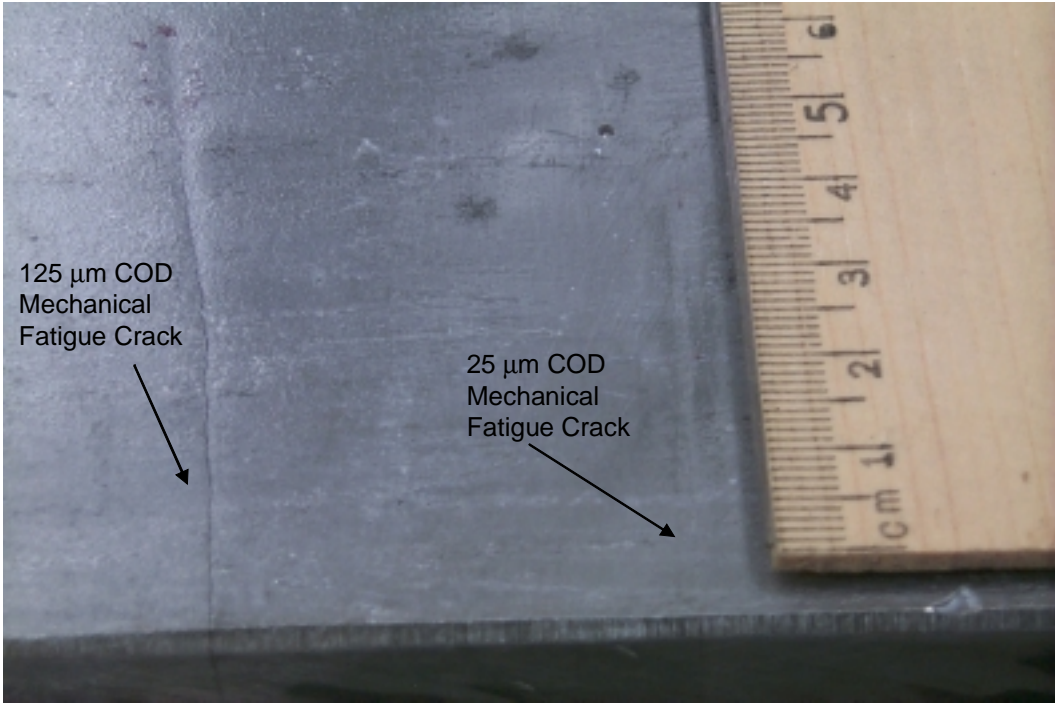


Figure A2 Two Mechanical Fatigue Cracks in Sample 4

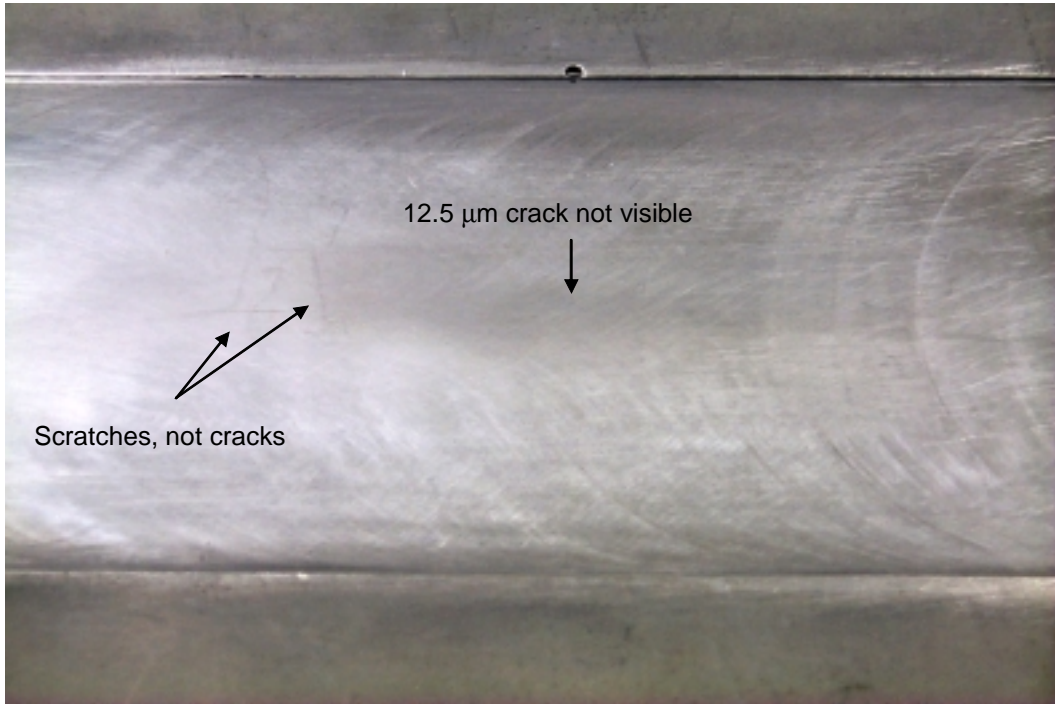


Figure A.3 Sample B118 Showing difficulty in Detecting a Thermal Fatigue Crack. With higher magnification, the crack is detectable, as shown in Figure 4.8

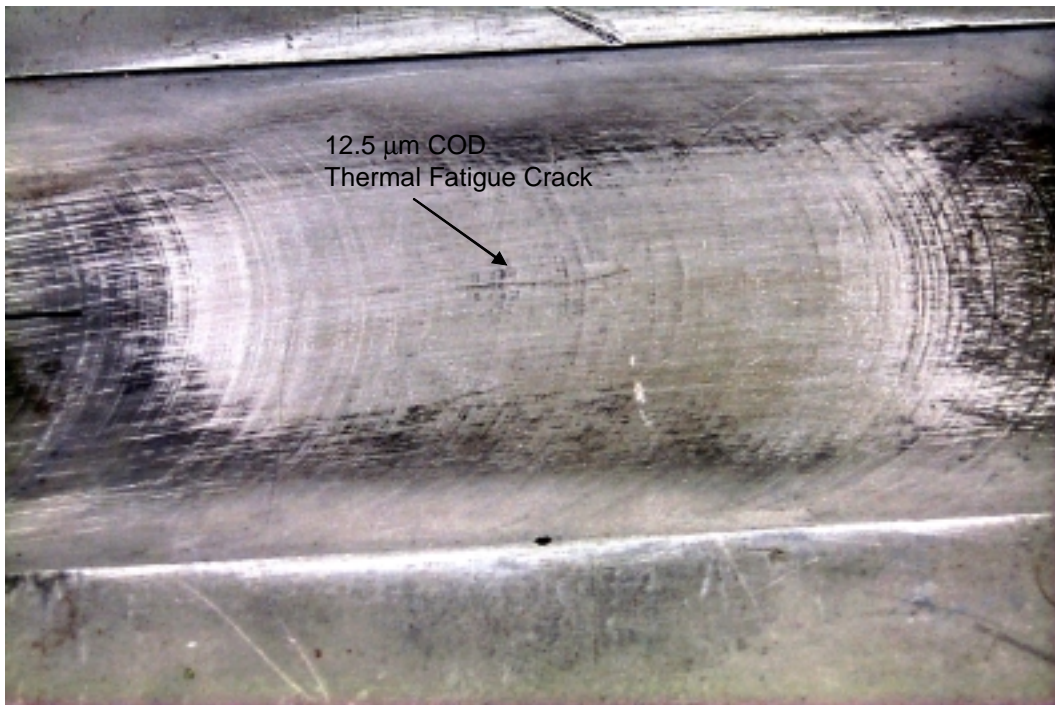


Figure A.4 Sample B117 Showing a 12- μm COD Thermal Fatigue Crack. This crack has a much higher contrast than the crack in sample B118, as the edge of the crack is chipped and discolored.

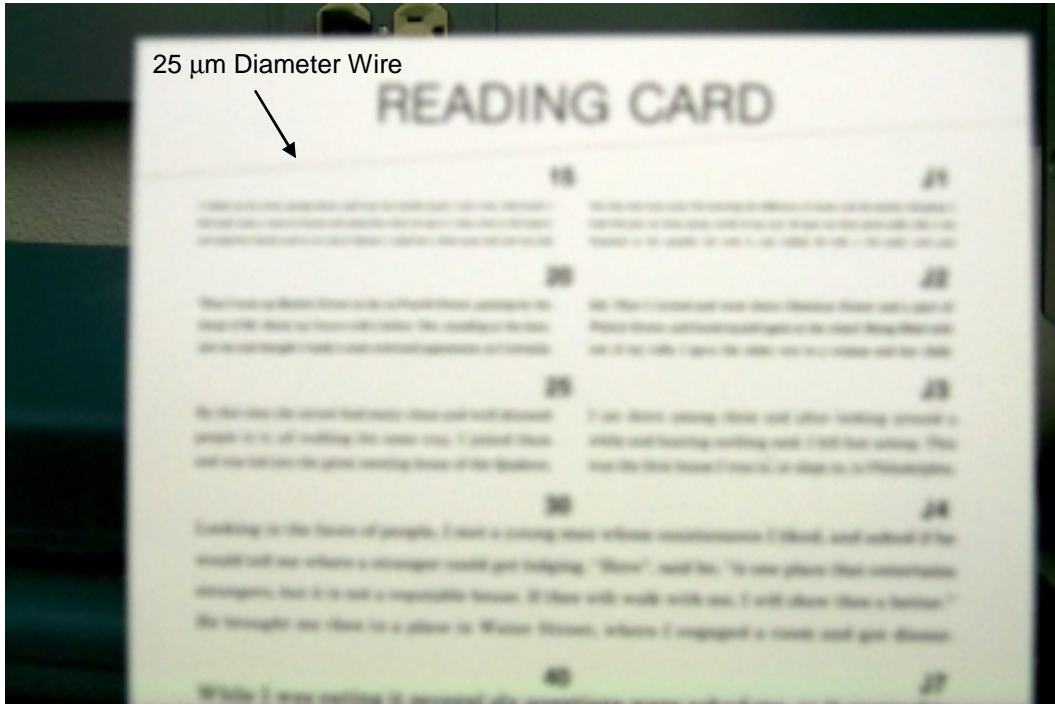


Figure A.5 Out-of-focus photo demonstrates that line detection is possible even with a very poorly functioning system.

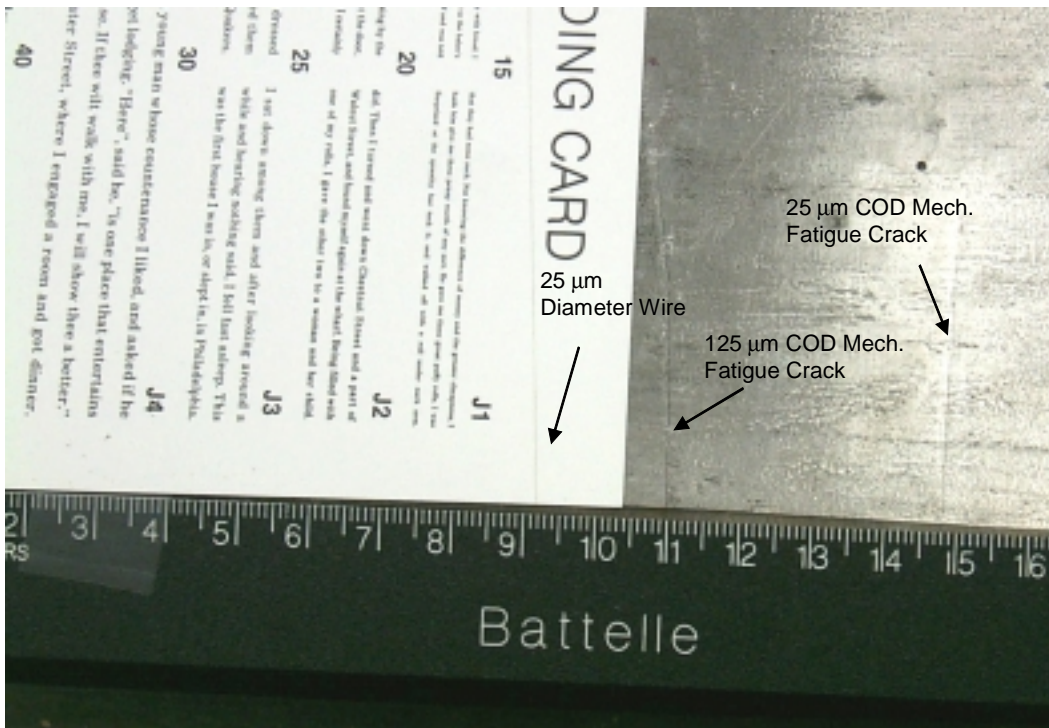


Figure A.6 Sample 4 with Jeager Reading Chart and a 25- μm Diameter Wire



Figure A.7 Frame Capture from Videotaped Visual Inspection of a Control Rod Drive Stub Tube Weld. Note the relatively soft focus.

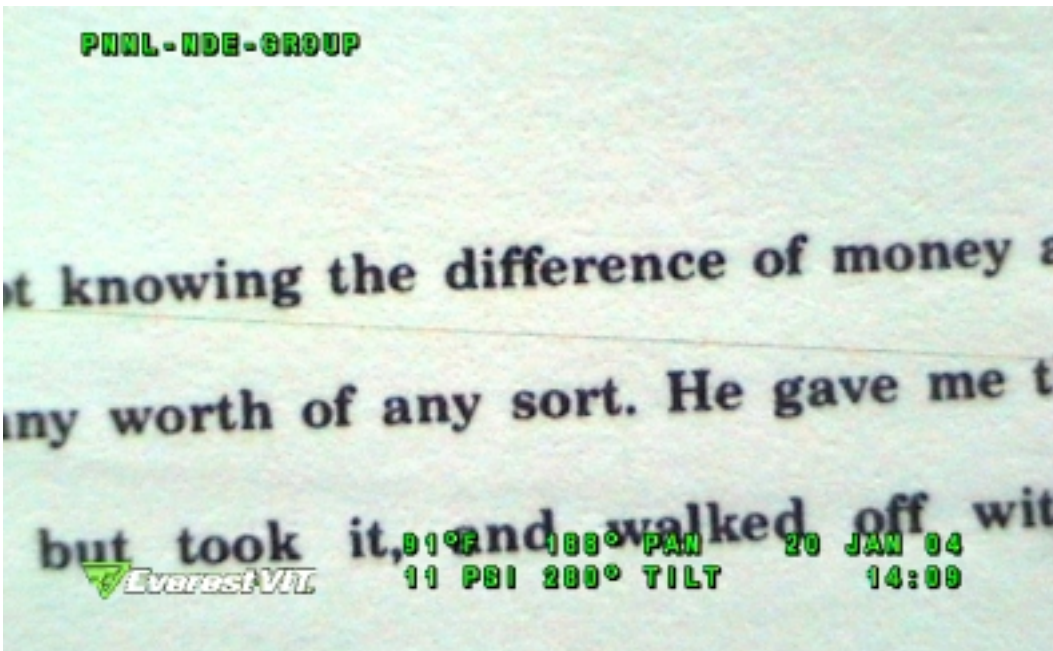


Figure A.8 Closeup of a Jeager Reading Chart and 25- μm Diameter Wire using CaZoom PTZ Camera. The wire is still less than 1 pixel wide.

APPENDIX B

Specifications for DIAKONT and EVEREST VIT Visual Testing Systems

Specifications for the DIAKONT RPV TV Inspection system

Minimum size of revealed defect	0.04 mm
Maximum speed of scanning	150 mm/sec
Operation distances range, mm	
in air	90-1500
in water	135-2000
Image	
in dynamic mode of inspection	Black-and-White
in static mode of inspection	color
IMAGE	
Resolution	600 TV lines
Signal/noise ratio:	
at normal conditions	56 dB
under dose rate 3×10^5 rad/h	47 dB
Focal length	13-139 mm
View angles by diagonal	Zoom
in air	5°-47°
in water	4°-36°
OPERATION CONDITIONS	
Operation environment	Water, Air
Transparency of environment	85%
Maximum operation temperature	
in air	40°C
in water	50°C
Atmospheric pressure	80-106 kPa
Hydrostatic pressure	100-270 kPa
Operation dose rate	3×10^5 rad/h
Integral dose	2×10^7 rad

Specifications for the Everest VIT CaZoom Inspection system

Type	Color 1/6" Super HAD™™ CCD (NTSC and PAL)
Resolution	470 HTV Lines
Zoom	25x optical, 12x digital for a total 300x Zoom
Focus	Automatic & manual
	Minimum Focal Distance: 800 mm in Telephoto, 35 mm in Wide Angle
Iris	Automatic & manual (f1.6 - close)
Electronic Shutter	Automatic & manual
Sensitivity	2.5 lux
Field Of View	2° Horizontal, 1.5° Vertical to 45° Horizontal 34° Vertical
Construction	Anodized aluminum
Lighting	
	2 lamps, 35 W each with focused dichroic reflectors
	35W flood: 16k lumens (1300cp) @ 30 deg (half angle) beam spread**
	35W spot: 75k lumens (6000cp) @ 10 deg (half angle) beam spread*8
	Turbo lamp mode: 88 watts
Optional	
	35W wide spot: 3000cp @ 20 deg (half angle) beam spread (Measured at 50% maximum intensity)
Camera Operating Environment	
	Temperature: -18 deg C to 49 deg C (0 deg F to 120 deg F)
Pressure	Waterproof to 45.0 m (150.0 ft) or 4.5 bar (65 PSI) external
Dose Rate	50Gy/hr (~5,000 R/hr)
Cumulative Dose	600 Gy (~60,000 R)